Toward resolution of the silicon dicarbide (SiC_2) saga: *Ab initio* excursions in the web of polytopism

Ida M. B. Nielsen and Wesley D. Allen[a)]
Department of Chemistry, Stanford University, Stanford, California 94305

Attila G. Császár
Department of Theoretical Chemistry, Eötvös University, H-1518 Budapest 112, P.O. Box 32, Hungary

Henry F. Schaefer III
Center for Computational Quantum Chemistry, University of Georgia, Athens, Georgia 30602

(Received 31 January 1997; accepted 16 April 1997)

The long-standing problem of the topography, energetics, and vibrational dynamics of the ground-state surface of SiC_2 is systematically investigated by means of the gamut of state-of-the-art electronic structure methods, including single-reference correlation techniques as extensive as the coupled-cluster singles and doubles method augmented by a perturbative triples term [CCSD(T)], the Brueckner doubles method (BD) with analogous contributions from both triple and quadruple excitations [BD(TQ)], and second- through fifth-order Møller–Plesset perturbation theory (MP2–MP5), as well as the multiconfigurational complete-active-space self-consistent-field [CASSCF(12,12)] approach. The one-particle basis sets for these studies ranged from Si$[6s4p1d]$, C$[4s2p1d]$ to Si$[7s6p4d3f2g1h]$, C$[6s5p4d3f2g1h]$. The methodological analysis resolves the polytopism problem regarding the mercurial potential energy surface for the circumnavigation of Si^+ about C_2^- in silicon dicarbide, whose topography is shown to exhibit almost all conceivable variations with level of theory. It is concluded that the $\tilde{X}\ ^1A_1$ global minimum of SiC_2 is a T-shaped (C_{2v}) structure connected monotonically to a linear transition state 5.8 kcal mol^{-1} higher in energy, thus ruling out any metastable linear isomer. Previously undocumented bent transition states and L-shaped minima are encountered at relatively high levels of theory, but ultimately these stationary points are shown to be spurious. High-level focal-point thermochemical analyses yield $D_0(\mathrm{Si–C_2})=151$ kcal mol^{-1}, and hence a substantial revision is made in the heat of formation, viz., $\Delta H^\circ_{f,0}(SiC_2)=+155$ kcal mol^{-1}. A complete quartic force field about the T-shaped minimum is determined at the CCSD(T) level with the aug-cc-pVTZ (Si$[6s5p3d2f]$, C$[5s4p3d2f]$) basis set and then employed in a preliminary probe of contours for large-amplitude motion, anharmonicity of the vibrations, and zero-point effects on the molecular structure. © *1997 American Institute of Physics.* [S0021-9606(97)01428-1]

A HISTORY OF CONUNDRUMS

In 1926 uncataloged bands near 5000 Å were discovered in the spectra of several carbon-rich stars by Merrill[1] and Sanford[2] at Mt. Wilson Observatory. Notwithstanding subsequent detailed investigations by McKellar[3] and Sanford,[4] the carrier of the electronic transitions was not identified until Kleman[5] reproduced the stellar bands in the laboratory some 30 years later by heating silicon in the graphite tube of a King furnace to optimal temperatures of 2300–2400 °C. On the basis of the complexity of the band system, the experimental conditions, and a partial vibrational analysis, the blue–green emission spectrum was tentatively ascribed to an Si–C–C species, assumed to be linear in analogy with the C_3 prototype. The strongest band at 4977 Å was assigned to the (000)–(000) transition.

Early mass spectrometric work[6] showed that gaseous SiC_2 evolves directly from solid silicon carbide at 2300 °C, and this process was used by Weltner and McLeod[7] in 1964 to trap the species in cryogenic matrices and probe it via infrared, visible, and near-ultraviolet spectroscopy. Flash discharge of phenylsilane also produces SiC_2, as exploited by Verma and Nagaraj[8] in 1974 to obtain the gaseous absorption spectrum in the 4300–5000 Å region. These studies[7,8] furthered the assignment of the Merrill–Sanford bands as $\tilde{X}\ ^1\Sigma^+/^1\Pi$ transitions of a linear SiC_2 molecule and established ground-state fundamental frequencies for C–C and Si–C stretching near 1742 and 852 cm^{-1}, respectively. However, the vibronic analyses required progressions antithetical to the Franck–Condon principle as well as stretching anharmonicities in the excited state anomalous in sign and magnitude. Disparate low-frequency bending fundamentals were also surmised: $(\nu_2'',\nu_2')=(300,230)$[7] versus (147, 145) cm^{-1}.[8] Verma and Nagaraj[8] mused the possible nonlinearity of one or both electronic states but preferred to implicate Fermi resonance interactions for the peculiar vibronic patterns, pending the unraveling of the rotational subbands to determine definitive molecular structures.

In a 1982 search for the elusive diatomic SiC radical, Bondybey[9] vaporized solid silicon carbide with a pulsed YAG laser, finding a predominance of atomic silicon

a)Current address: Center for Computational Quantum Chemistry, University of Georgia, Athens, GA 30602.

and SiC_2 instead, *inter alia*. Time-resolved laser-induced fluorescence spectroscopy was used to interrogate SiC_2 in both a neon matrix and a cold gas stream. Bondybey noted that the shape of SiC_2 is not *a priori* obvious, given the exceedingly flat bending potential of the isovalent C_3 analog ($\nu_2 = 64\ cm^{-1}$)[10] and the reluctance of silicon to form π bonds; but in reassigning the Merrill–Sanford system, the earlier assumptions of linearity were retained, in conformity with Walsh's rules. A hot band displaced 354 cm^{-1} from the origin ($T_0 = 20\,070\ cm^{-1}$) was ascribed to $2\nu_2''$, and satellite bands appearing 455 cm^{-1} above the most active ν_3' progression were attributed to the $2\nu_2'$ interval. The troublesome bending fundamentals were thus assigned as $(\nu_2'', \nu_2') = (175\,228)\ cm^{-1}$.

Ab initio electronic structure theory was first applied to the silicon dicarbide puzzle in 1983[11] by means of the restricted Hartree–Fock self-consistent-field (SCF) formalism with basis sets of up to double-ζ plus polarization (DZP) quality. In accord with previous experimental interpretations, the ground electronic state ($\tilde{X}\ ^1\Sigma^+$) was predicted to have a highly ionic, linear $Si^+–C{\equiv}C^-$ structure with a dipole moment of 4.8 D, while a much more covalent $^1\Pi$ linear state was located approximately 2.5 eV higher in energy. The possibility of a competitive CSiC isomer was excluded. Although the SCF stretching frequencies of the $\tilde{X}\ ^1\Sigma^+$ state were in unusually poor agreement with experiment, they were not deemed inconsistent with the assignments of Verma and Nagaraj.[8]

The breakthrough in the silicon dicarbide saga was realized less than a year later by means of a notable synergy between laser spectroscopists at Rice and *ab initio* theorists at Berkeley. In the Rice experiments, Michalopoulos, Geusic, Langridge-Smith, and Smalley (MGSS)[12] prepared a beam of cold SiC_2 by laser vaporization of a silicon carbide rod followed by entrainment in a helium carrier gas and supersonic expansion into a vacuum. Resonant two-photon ionization (R2PI) in a time-of-flight mass spectrometer was used to pinpoint 32 rotational transitions between the ground vibrational states of the 4977 Å band system. Analysis of the R2PI spectrum in terms of $\tilde{X}\ ^1\Sigma^+ \rightarrow {}^1\Pi$ transitions was found to require untenable bond lengths and an unusually large lambda doubling parameter for the upper state. Alerted to this conflict, Grev and Schaefer[13] at Berkeley discovered that at the DZP SCF level of theory the linear $\tilde{X}\ ^1\Sigma^+$ minimum of SiC_2 connects to a cyclic (C_{2v}) saddle point only 5.1 kcal mol^{-1} higher in energy. Subsequent single-point DZP configuration interaction singles and doubles (CISD) computations actually placed the cyclic form 0.4 kcal mol^{-1} *below* the linear structure, and additional *d*-type polarization functions were shown to stabilize the highly strained ring further. A final prediction of ΔE (ring−linear) $= -5$ kcal mol^{-1} was advanced accordingly. Meanwhile, the Rice group[12] fitted asymmetric-top rotational constants to their data and deduced the C_{2v} parameters [r_0(Si–C), r_0(C–C)] (Å) = (1.812, 1.250) and (1.881, 1.304) for the lower and upper states, respectively, the former distances being in remarkable agreement with the structure of the *ab initio* cyclic stationary point.[13] Therefore, it was at last revealed that the 4977 Å band system arises from $\tilde{X}\ ^1A_1/\tilde{A}\ ^1B_2$ transitions of an SiC_2 ring, in which the low-lying upper state is formed by an in-plane $\pi \rightarrow \pi^*$ excitation within the weak, highly strained, carbon–carbon triple bond. Ample evidence from the details of the R2PI spectrum confirmed this interpretation: the electronic transition is polarized along the inertial *b* axis, and the odd/even *K* levels in the lower/upper (000) vibronic manifolds are absent, as expected for $\tilde{X}\ ^1A_1$ and $\tilde{A}\ ^1B_2$ electronic states with equivalent carbon nuclei of zero spin.

THE PROLIFERATION OF DEFINITIVE SPECTROSCOPY

The conclusions resulting from the R2PI experiments[12] of 1984 ignited a proliferation of detailed spectroscopic work on SiC_2. Thaddeus *et al.*[14] immediately assigned nine new lines in the millimeter wave spectrum of the evolved carbon star IRC+10216 to $^{28}SiC_2$ and estimated temperatures and mean column densities of this species in the circumstellar environment. Improved rotational constants were determined, incorporating the effects of centrifugal distortion, and a revised structure was extracted. Within two years, continuing searches of the IRC+10216 envelope uncovered more SiC_2 signals, including the $1_{01} \rightarrow 0_{00}$ line at 1.27 cm which was the first probe of the ground rotational state,[15] and six millimeter wave emissions due to the ^{29}Si and ^{30}Si isotopomers.[16]

The compilation of definitive spectroscopy on SiC_2 continued with renewed matrix-isolation Fourier transform infrared experiments.[17–19] In 1985 Shepherd and Graham[17] observed that only four new symmetric stretching fundamental bands result from ^{13}C substitutions, viz., ν_1(C–C str.) at (1708, 1674) cm^{-1} and ν_2(Si–C str.) at (815, 805) cm^{-1}, indicating equivalent carbon nuclei in SiC_2. A normal coordinate analysis was found to yield reasonable force constants for C_{2v} structures with vertex angles near 40°, but not for linear frameworks. In a brief 1988 note[18] these authors commented on several implications of the matrix isolation studies: (a) under the modified (C_{2v}) selection rules, the 354 cm^{-1} interval of Bondybey[9] gives $\nu_3 \approx 180\ cm^{-1}$; (b) because the quadratic force constants f_{rr} and $f_{rr'}$ for Si–C stretching are comparable, the molecule is best considered a T-shaped $Si^+C_2^-$ species; (c) the C–C distance and stretching fundamentals for C_2^- (1.268 Å, 1758 cm^{-1})[20] and SiC_2 (1.268 Å, 1742 cm^{-1}) are almost identical, bolstering the ionic bonding model; and (d) to avert assignment of an unprecedented argon matrix shift, the $\tilde{A}\ ^1B_2 \rightarrow \tilde{X}\ ^1A_1$ gaseous emission spectrum of Kleman[5] must be reinterpreted to give $\nu_2(a_1$ Si–C str.) = 837 rather than 852 cm^{-1} for the ground state. Finally, in a 1990 investigation[19] the highly anharmonic $\nu_3(b_2)$ vibration was located directly for the first time in the far-infrared region by FTIR spectroscopy, appearing in argon matrices at 160.4, 157.7, and 155.3 cm^{-1} for $^{28}Si^{12}C_2$, $^{28}Si^{12}C^{13}C$, and $^{28}Si^{13}C_2$, respectively. A Jacobi-type force field was found to provide the most favorable fit to

the isotopomeric frequency data, consistent with a T-shaped molecule exhibiting a nondirectional Si–C_2 bond.

High-resolution rotational spectroscopy of SiC_2 was not achieved in the laboratory until 1988, but within a few years a flurry of activity catalogued myriad transitions in the gas phase. First, Bredohl *et al.*[21] generated the Merrill–Sanford system by flash-discharge techniques and unraveled numerous K'/K'' subbands, analyzing 646 and 482 lines in the (000)–(000) and (010)–(000) vibronic manifolds, respectively, on the basis of the Watson *A*-reduced Hamiltonian. The fit provided $[r_0(\mathrm{C–C}),\ r_0(\mathrm{Si–C})]=(1.2649,\ 1.8362)$ Å and (1.3295, 1.9021) Å for the $\tilde{X}\ ^1A_1$ and $\tilde{A}\ ^1B_2$ states, respectively, as well as $T_0=20\,085.505\ \mathrm{cm}^{-1}$ and $\nu_2'=435.038\ \mathrm{cm}^{-1}$. Subsequently, Gottlieb, Vrtílek, and Thaddeus[22] identified 41 *a*-type transitions ($K_a\leqslant 10$, $13\leqslant J\leqslant 17$) in the pure rotational spectrum of $\tilde{X}\ ^1A_1$ SiC_2 from a $SiH_4/C_2H_2/CO$ discharge, the same technique which produced the long-sought SiC radical.[23] Both quartic and sextic centrifugal distortion constants were extracted from an *A*-reduced Hamiltonian fit, while a gas-phase frequency $\nu_3=186\pm 11\ \mathrm{cm}^{-1}$ was deduced from the inertial defect in the rotational constants. The burgeoning database was also supplemented by Suenram, Lovas, and Matsumura,[24] who used a laser-ablation source to locate the $1_{01}-0_{00}$ line of $^{28}SiC_2$ at 23 600.242 MHz and found a dipole moment of 2.393(6) D by measuring the Stark effect on this transition. In 1991 several collaborators[25,27] undertook an astronomical and laboratory study of $Si^{13}CC$ to determine the $^{12}C/^{13}C$ isotopic ratio in IRC+10216 as a probe of stellar mixing and dredge-up processes. Microwave data for $^{28}SiC_2$, $^{29}SiC_2$, $^{30}SiC_2$, and $^{28}Si^{13}C^{12}C$ were compiled, from which the Kraitchman equations gave the substitution structure $[r_s(\mathrm{C–C}),\ r_s(\mathrm{Si–C})]=[1.268\ 55(36),\ 1.832\ 32(58)]$ Å, exhibiting accord with various r_0 structures[14,21,24] and typical agreement with theory,[13] but revealing that the earliest R2PI bond distances[12] were too small because of erroneous wavelength calibration.

The pure rotational spectrum of the ν_3 excited vibrational state of SiC_2 was analyzed in related work by Bogey *et al.*,[26,27] who identified 95 lines in the ($1\leqslant K_a\leqslant 13$, $8\leqslant J\leqslant 21$) interval. Evidence for large-amplitude motion abounded. In particular, the rotational levels could not be fit to experimental accuracy even with centrifugal distortion terms through eighth order; the vibration–rotation interaction constants $\alpha_3^B=167$ MHz and $\alpha_3^C=229$ MHz were found to be an order of magnitude larger than in typical semirigid molecules; and the inertial defect ($\Delta=1.19$ u Å^2) exhibited by the ν_3 state was extreme. Coudert[28] developed a model Hamiltonian to account for the large-amplitude ν_3 mode and achieved improved rotational fits, although the potential energy function extracted from the analysis was deficient in several respects. Einstein *A*-coefficients and mean lifetimes for rotational levels in the v_3 state were computed by Chandra and Sahu[29] in 1993. Finally, in 1994 Izuha, Yamamoto, and Saito[30] investigated the rotational spectrum of SiC_2 in both the ν_3 and $2\nu_3$ excited vibrational states, recording with improved accuracy 48 and 23 *a*-type *R*-branch lines, respectively, in these manifolds. Sextic, octic, and decatic centrifugal distortion parameters were required to fit the observed frequencies within experimental errors. The vibrational dependence of both the inertial defect and the quartic centrifugal distortion constants proved to be pronounced and nonlinear for the large-amplitude ν_3 mode, although a simple anharmonic model satisfactorily explained this behavior.

Extensive gas-phase spectroscopic probes of the full vibrational eigenspectrum of the $\tilde{X}\ ^1A_1$ and $\tilde{A}\ ^1B_2$ electronic states have also been executed since 1990. As a first step, Fantoni and collaborators[31] assimilated copious information from early work on the Merrill–Sanford band system and augmented it with coherent anti-Stokes Raman scattering (CARS) data from flow-reactor experiments to derive values for most of the anharmonicity constants χ_{ij} of the $\tilde{X}\ ^1A_1$ and $\tilde{A}\ ^1\,^1B_2$ states. Shortly thereafter Butenhoff and Rohlfing[32] reported authoritative work at Sandia on the laser-induced fluorescence (LIF) excitation and dispersed fluorescence (DF) spectra of the $\tilde{X}\ ^1A_1\rightarrow\tilde{A}\ ^1\,^1B_2$ system of jet-cooled SiC_2, including rotational analyses of several previously unobserved bands. Discovery of the 3_0^1 transition 487 cm^{-1} above the band origin ended longstanding confusion and sparked further reassignment of the $\tilde{A}\ ^1\,^1B_2$ vibronic structure, while a joint analysis of the 3_1^1 hot band revealed that $\nu_3''=196.37\ \mathrm{cm}^{-1}$, or $36\ \mathrm{cm}^{-1}$ above its argon matrix counterpart.[19] The DF spectra proved to be rich sources of vibrational term energies for the $\tilde{X}\ ^1A_1$ state, yielding 43 levels in all. Most notably, a long $(0,0,\nu_3'')$ progression for $\nu_3''=1$ to 16 exhibits extreme negative anharmonicity, as well as periodic Fermi-resonance perturbations evidencing strong coupling between the ν_2'' and ν_3'' vibrational modes. In contrast, the $(v_1'',v_2'',0)$ states are very regular and are reckoned nicely by the vibrational constants $\omega_1=1756.8$, $\omega_2=844.0$, $\chi_{11}=-11.8$, $\chi_{22}=-4.58$, and $\chi_{12}=-3.8\ \mathrm{cm}^{-1}$. Moreover, all three vibrational modes of the $\tilde{A}\ ^1\,^1B_2$ state are quite harmonic, the 19 LIF band origins being fit well by a Dunham expansion with coefficients $\omega_1=1475.8$, $\omega_2=456.3$, $\omega_3=488.0$, $\chi_{11}=-14.0$, $\chi_{22}=-1.8$, $\chi_{33}\approx 0.3$, $\chi_{12}=13.9$, $\chi_{13}=17.1$, and $\chi_{23}=-12.4\ \mathrm{cm}^{-1}$.

The vibrational analyses of SiC_2 culminated in a 1994 collaboration between Ross and the Sandia group.[33] Stimulated emission pumping (SEP) of the $\tilde{X}\ ^1A_1/\tilde{A}\ ^1B_2$ system was implemented to dissect the $(0,0,\nu_3'')$ manifolds for $\nu_3''=2$, 4, 6, 12, and 14 with full rotational resolution, providing a collection of 11–15 $J_{K_aK_c}$ levels for each of these large-amplitude bending states. These new results were combined with existing vibrational term values[32] and microwave lines[22,26] and globally fit to a semirigid bender Hamiltonian (SRB)[34] with reasonable accuracy. In this dynamical model, SiC_2 was treated in essence as a molecular pinwheel, in which the C_2 moiety spins about its center of mass while the silicon spectator wobbles about its equilibrium position. The range of Si–C_2 Jacobi angles (ρ) sampled by the experimental vibrational levels involved in the analysis extended to within 30° of linearity. The minimum energy path and potential energy function derived from the SRB fit extrapolated to a linear SiC_2 structure which was merely a transition state

for the interconversion of equivalent T-shaped minima lying 1883 cm^{-1} lower in energy; however, a shallow linear minimum could not be ruled out completely due to the lack of explicit spectroscopic data for $\rho < 30°$.

THE PERSISTENT CHALLENGE FOR *AB INITIO* THEORY

In the aftermath of the silicon dicarbide structure elucidation in 1984,[12,13] *ab initio* theory was presented with a challenge which proved to be almost insuperable: achieving *converged* predictions of a T-shaped global minimum with correct surface curvature, determining unassailably whether a low-lying linear isomer exists, and establishing the topography for the large-amplitude pinwheel motion. Pauzat and Ellinger[35] focused on the structure and spectroscopy of the linear $^1\Sigma^+$ state, predicting it to be a metastable isomer via triple-ζ plus polarization (TZP) configuration interaction (CI) computations based on projected localized orbitals. Their vibrational analysis, which included diagonal anharmonicity in the normal coordinate space, gave harmonic bending frequencies at the SCF and CI levels of 125 and 838 cm^{-1}, respectively, the latter being suspiciously high. In one-dimensional bending searches at the [Si($6s5p1d$)/C($5s4p1d$)] MP4 level, Oddershede *et al.*[36] found a shallow linear well of 0.4 kcal mol^{-1} depth lying 0.84 kcal mol^{-1} above the T-shaped minimum. They characterized silicon dicarbide as a polytopic[37] $Si^+C_2^-$ species with nondirectional ionic bonding, similar to KCN, which is known from microwave studies[38] to be L-shaped in the gas phase. Second-order polarization propagator calculations of numerous excitation energies showed that the linear and T-shaped forms have clearly distinguishable electronic spectra. It was concluded that both forms of SiC_2 should be observable under high temperature conditions.

Fitzgerald, Cole, and Bartlett[39] applied analytic first and second derivative techniques for second-order many-body perturbation theory [MBPT(2)] to the SiC_2 problem by means of a DZP basis, obtaining the bending frequencies ω_3(ring)=183 and ω_2(linear)=147 cm^{-1}, i.e., both structures are minima at this level of theory. The energy difference between the two isomers oscillated as the perturbation series was extended, and due to a large triples stabilization (2.8 kcal mol^{-1}) the linear form was actually placed by the DZP MBPT(4) method 1.36 kcal mol^{-1} *lower* than the T-shaped ring isomer. However, basis set improvements and further triples corrections, as implemented by the ($6s4p1d$) CCSD+T(CCSD) approach, returned ΔE (ring $-$linear) to -1.60 kcal mol^{-1}.

A timely study of the methodological dependence of ΔE (ring$-$linear) was completed by Sadlej and co-workers in 1988.[40] Basis sets ranging from [Si($8s6p$)/C($5s3p$)] to [Si($8s6p2d1f$)/C($5s3p2d1f$)], some partially optimized, were employed in conjunction with the SCF, MBPT(2-4), CCSD, and CCSDT-1a methods. It was documented that (a) with carefully constructed basis sets, even SCF wave functions predict the T-shaped (ring) form as the lowest structure; (b) notwithstanding the ionic nature of SiC_2, diffuse orbitals on carbon have little effect on the relative energy; (c) the addition of f functions provides a critical stabilization (1.5 kcal mol^{-1}) of the ring isomer; and (d) the relative lowering of the linear form by triple excitations remains substantial (2.3 kcal mol^{-1}) in iterative procedures. The problem posed by ΔE (ring$-$linear) for SiC_2 [or Δ(T–L) henceforth] was clearly enunciated in the closing remarks of the authors: ''In summary, we have shown that a definitive theoretical prediction of Δ(T–L) for SiC_2 would require a highly correlated calculation, most likely by methods like CCSDT. Also, it is necessary to use rather large basis sets, probably not less than 150 CGTOs. Cancellation effects prevent the use of different size basis sets for the SCF and the correlated calculation. The 'final' determination of Δ(T–L) for SiC_2 will thus remain a challenge for theoreticians for a while.''

This challenge has essentially remained unanswered, despite scattered theoretical work since 1988. In the aforementioned 1994 collaboration,[33] Rohlfing added new results to the *ab initio* compilation. Of greatest significance, QCISD/6-311+G($3df$) theory predicted ω_2(linear)=76i cm^{-1}, ω_3(ring)=152 cm^{-1}, and Δ(T–L) $=-5.2$ kcal mol^{-1}, in support of the semirigid bender analysis of the SiC_2 rovibrational levels, which indicated that the linear form is merely a transition state 5.4 kcal mol^{-1} above the T-shaped minimum. Within three months Deutsch and Curtiss[41] revisited the Δ(T–L) question with the aid of G2 theory.[42] This thermochemical scheme, whereby relatively high-level *ab initio* computations are calibrated empirically, yielded Δ(T–L)$=-3.51$ kcal mol^{-1}, as well as an atomization energy (294.7 kcal mol^{-1}) which refined the empirical heat of formation of $SiC_2(\tilde{X}\ ^1A_1)$. Additivity approximations[43] assumed in G2 theory were demonstrated to give inconsequential errors in the case of SiC_2. Moreover, the remarkable agreement reported by Ross *et al.*[33] between theory and experiment for Δ(T–L) was shown to be only an advantageous consequence of the neglect in the QCISD/6-311+G($3df$) method of the large triples stabilization of the linear form. Finally, two relatively recent studies have provided some limited information on CSiC isomers of silicon dicarbide.[44,45] In particular, linear CSiC, whether a local minimum[44] or saddle point,[45] connects to a highly bent (noncyclic) C_{2v} minimum roughly 50 kcal mol^{-1} lower in energy, but this bent structure lies at least 80 kcal mol^{-1} above the global T-shaped SiC_2 minimum.

THEORETICAL PROSPECTUS AND PROCEDURES

The multifaceted challenge to theory posed by the SiC_2 species is the stimulus of the current study. The first goal is to systematically reveal the remarkable variation with level of theory of even the most qualitative features of the potential energy surface of $\tilde{X}\ ^1A_1$ SiC_2 by cataloging geometric structures, harmonic vibrational frequencies, and relative energies for various types of stationary points. The appearance and subsequent disappearance of previously uncharacterized bent and L-shaped structures on the Si–C_2 pinwheel surface is of particular concern. The extensive, present work documents the requirements for a definitive *ab initio* mapping of

the surface for large-amplitude bending, clarifies the conflicting results from previous theoretical studies, and further elevates SiC_2 as a testing ground for methodological development. The second goal of this investigation is to determine the barrier to linearity and the heat of formation of $\tilde{X}\ ^1A_1$ SiC_2 by means of the highest possible levels of *ab initio* theory. These predictions constitute substantial improvements over the best experimental results for these thermochemical quantities. Moreover, the question of the existence of a metastable linear isomer of SiC_2 is resolved. The final aspect of this study entails the determination of a complete quartic force field for anharmonic vibrations, from which standard spectroscopic constants from second-order rovibrational perturbation theory are computed and an r_e structure of SiC_2 is derived from high-resolution microwave measurements of isotopomeric (A_0,B_0,C_0) sets. Identification is made of the aspects of this approach which are problematic.

The atomic Gaussian-orbital basis sets employed in this study are denoted as DZ(d), TZ($2d$), TZ($2d1f$), cc-pVXZ, and aug-cc-pVTZ. In the first three designations of the form $A(x)$, A is descriptive of the underlying sp basis [DZ, TZ=double- and triple-ζ], and x specifies the number and types of polarization functions appended to all atoms. The DZ basis consists of the C($9s5p$) and Si($11s7p$) primitives of Huzinaga[46] and the C($4s2p$), Si($6s4p$) contractions of Dunning.[47,48] The TZ basis involves the same C($9s5p$), Si($11s7p$) primitives contracted to C($5s3p$) and Si($7s5p$) according to Dunning.[47,48] The polarization-function exponents employed in the DZ(d) basis are $\alpha_d(\mathrm{C})=0.750$ and $\alpha_d(\mathrm{Si})=0.500$, which are representative optimal exponents for uncorrelated wave functions.[49] The polarization functions used in the TZ($2d$) set were obtained by splitting the above d exponents with a bifurcation factor of 2, yielding $\alpha_d(\mathrm{C})=(0.375, 1.500)$ and $\alpha_d(\mathrm{Si})=(0.250, 1.000)$. The TZ($2d1f$) set was constructed by adding to the TZ($2d$) basis f manifolds with exponents $\alpha_f(\mathrm{C})=0.700$ and $\alpha_f(\mathrm{Si})=0.550$. In the aforementioned basis sets, Cartesian d and f manifolds were used, i.e., supernumerary s and p contaminants were not excluded. The cc-pVXZ basis sets [X=D (double), T (triple), Q (quadruple), or 5 (quintuple)] are the correlation-consistent constructions of Dunning.[50,51] The contractions are C($9s4p1d/3s2p1d$), Si($12s8p1d/4s3p1d$) for cc-pVDZ; C($10s5p2d1f/4s3p2d1f$), Si($15s9p2d1f/5s4p2d1f$) for cc-pVTZ; C($12s6p3d2f1g/5s4p3d2f1g$), Si($16s11p3d2f1g/6s5p3d2f1g$) for cc-pVQZ; and C($14s8p4d3f2g1h/6s5p4d3f2g1h$), Si($20s12p4d3f2g1h/7s6p4d3f2g1h$) for cc-pV5Z. The aug-cc-pVTZ basis is formed by appending to the cc-pVTZ basis diffuse ($1s1p1d1f$) shells with exponents optimized for the atomic anions.[51,52] The d and f manifolds in the cc-pVXZ basis sets are comprised only of pure angular momentum functions. The various basis sets employed in this study range in number of contracted Gaussian functions from 56 in the DZ(d) case to 277 for the cc-pV5Z set.

Reference electronic wave functions were determined by the single-configuration restricted Hartree–Fock method (RHF)[53–55] and by the complete-active-space self-consistent-field approach (CASSCF).[56] The CASSCF computations involved the full valence active space, 12 electrons in 12 orbitals, as indicated hereafter by the suffix (12,12). Dynamical electron correlation was accounted for by Møller–Plesset perturbation theory from second through fifth order [MP2, MP3, MP4(SDTQ), and MP5(SDTQ)],[57–61] by the single-reference, configuration interaction singles and doubles method (CISD),[62–64] by the coupled cluster singles and doubles method (CCSD),[65–70] by the CCSD method augmented by a perturbative contribution from connected triple excitations [CCSD(T)],[71,72] and by the Brueckner doubles method (BD)[73] with analogous corrections for both triple and quadruple excitations [BD(T) and BD(TQ)].[61,73,74] Some CISD predictions were corrected for the effect of unlinked quadruple excitations by applying the Davidson correction.[75] Energies thus obtained are denoted as CISD+(Q). The carbon $1s$ and the silicon $1s$, $2s$, and $2p$ core orbitals were excluded from the active space in all correlation treatments, in accord with the findings of Sadlej and co-workers.[40] No virtual orbitals were frozen. The electronic structure computations reported here were performed with the program packages PSI,[76] GAUSSIAN 92,[77] and GAMESS.[78]

Geometry optimizations were performed with analytic gradient techniques[79–83] for the RHF, CASSCF, MP2, CISD, CCSD, and CCSD(T) methods, whereas energy points alone were used for the MP3, MP4(SDTQ), MP5(SDTQ), BD, BD(T), and BD(TQ) optimizations. For methods where analytic gradients were available, the maximum component of the gradient was smaller than 10^{-6} a.u. at all stationary points, whereas this threshold was relaxed to 10^{-4} a.u. for methods where gradients were computed numerically. To characterize the stationary points, harmonic vibrational frequencies were computed at all optimized geometries. Analytic second-derivative techniques were employed in the RHF[79,84,85] and MP2[86,87] cases, while CASSCF, CISD, CCSD, and CCSD(T) second derivatives were obtained by finite differences of analytic gradients. In the MP3, MP4(SDTQ), MP5(SDTQ), BD, BD(T), and BD(TQ) cases, second derivatives were obtained by double-finite difference procedures.[88] In all cases, the displacement sizes were 0.01 Å or 0.02 rad for symmetrized internal coordinates.

The complete quartic force field of $\tilde{X}\ ^1A_1$ SiC_2 was computed at the aug-cc-pVTZ CCSD(T) level of theory by taking finite differences of 18 gradient points[88] obtained from single and double displacements around the T-shaped minimum located at this level of theory. Symmetrized internal coordinates $S_1=r(\mathrm{C–C})$, $S_2=2^{-1/2}[r_1(\mathrm{Si–C})+r_2(\mathrm{Si–C})]$, and $S_3=2^{-1/2}[r_1(\mathrm{Si–C})-r_2(\mathrm{Si–C})]$ were displaced in positive and negative steps of 0.005 Å (S_1 and S_2) or 0.01 Å (S_3). The high accuracy of the numerical differentiation procedure was confirmed for many force field elements by comparison with force constants computed from energy points alone.

ANALYSIS OF THE POLYTOPISM PROBLEM

The consensus emerging from the multitude of theoretical and spectroscopic investigations reviewed above is that SiC_2 is an ionic species exhibiting nondirectional bonding

TABLE I. Optimum geometric structures of SiC_2 species.[a]

Method	Linear ($^1\Sigma^+$)		Bent ($^1A'$)			L-shaped ($^1A'$)			T-shaped ($^1A_1$)	
	r_e(Si–C)	r_e(C–C)	r_e(Si–C)	r_e(C–C)	θ_e(Si–C–C)	r_e(Si–C)	r_e(C–C)	θ_e(Si–C–C)	r_e(Si–C)	r_e(C–C)
DZ(d) RHF	1.6756	1.2727	1.6768	1.2711	114.50	1.6831	1.2689	102.11	1.8347	1.2556
DZ(d) CASSCF(12,12)	1.7179	1.3137		b			b		1.8501	1.2947
DZ(d) MP2	1.7056	1.3027	1.7029	1.3053	132.13		c		1.8365	1.2955
DZ(d) MP3	1.6908	1.2903	1.6896	1.2925	135.85	1.7346	1.2854	82.81	1.8349	1.2802
DZ(d) MP4	1.7129	1.3162	1.7103	1.3157	110.36		c		1.8445	1.3007
DZ(d) MP5	1.6971	1.2953	1.6969	1.2991	134.03		c		1.8410	1.2877
DZ(d) CISD	1.6869	1.2881	1.6857	1.2899	129.38	1.7259	1.2823	84.22	1.8336	1.2759
DZ(d) CCSD	1.6939	1.2953	1.6935	1.2982	130.95		c		1.8381	1.2855
DZ(d) CCSD(T)	1.7056	1.3056	1.7055	1.3086	118.40		c		1.8447	1.2934
DZ(d) BD	1.6928	1.2941	1.6921	1.2969	133.15	1.7705	1.2866	76.60	1.8371	1.2850
DZ(d) BD(T)	1.7057	1.3052	1.7053	1.3084	119.77		c		1.8449	1.2936
DZ(d) BD(TQ)	1.7016	1.3028	1.7018	1.3065	126.48		c		1.8430	1.2930
TZ(2d) RHF	1.6740	1.2604		c		1.6892	1.2588	100.12	1.8420	1.2467
TZ(2d) CISD	1.6874	1.2710		c		1.7182	1.2682	89.55	1.8434	1.2597
TZ(2d) CCSD	1.6954	1.2781		c		1.7479	1.2734	83.14	1.8497	1.2684
TZ(2d) CCSD(T)	1.7081	1.2889		b		1.7508	1.2830	84.54	1.8573	1.2767
TZ(2d1f) RHF	1.6689	1.2614	1.6691	1.2614	158.87	1.6873	1.2586	98.36	1.8335	1.2461
aug-cc-pVTZ CCSD(T)	1.7057	1.2920		b			c		1.8534	1.2798

[a]Bond distances in Å, bond angles in degrees.
[b]Optimization was not attempted.
[c]Not a stationary point at the given level of theory.

between Si^+ and C_2^- fragments. It is certain that the potential energy surface for pinwheel motion of the C_2^- moiety in the presence of the Si^+ spectator is exceedingly flat. Such a property was originally termed ''polytopic'' by Clementi, Kistenmacher, and Popkie[37] in describing the circumnavigation of Li^+ about CN^- in gaseous lithium cyanide. The polytopic bonding in SiC_2 requires *ipso facto* that all electronic structure subtleties resulting from continuing reorientation of the C_2^- polarization by Si^+ be recovered completely for any theoretical treatment to be reliable. The failure of a host of *ab initio* methods to escape this web constitutes the ''polytopism problem.'' Indeed, the SiC_2 pinwheel surfaces given by the gamut of traditional theoretical techniques exhibit almost all conceivable topographies.

The methodological analysis of the polytopism problem is begun here by surveying the full set of correlation treatments [RHF, CASSCF(12,12), MP2, MP3, MP4, MP5, CISD, CCSD, CCSD(T), BD, BD(T), and BD(TQ)] with the modest DZ(d) basis set. Next, the series TZ(2d) and TZ(2d1f) RHF, TZ(2d) CISD, TZ(2d) CCSD, and TZ(2d) CCSD(T) is implemented. The detailed searches on the polytopic surface culminate with the aug-cc-pVTZ CCSD(T) method. Optimized geometric structures, total and relative energies, and harmonic vibrational frequencies for all of these levels of theory are given in Tables I–III. As depicted in Fig. 1, four distinct types of stationary points are encountered: (a) linear ($C_{\infty v}$); (b) bent (C_s), with obtuse angles θ(Si–C–C)>105°; (c) L-shaped (C_s), with θ(Si–C–C)=90°±15°; and (d) ring or T-shaped (C_{2v}), with θ(Si–C–C) near 70°. At lower levels of theory, explicit searches for other structures were carried out either by scanning the θ(Si–C–C) potential for fixed bond lengths or by starting geometry optimizations between known stationary points. No other types of stationary points were located, however.

The extent to which the basic topography of the SiC_2 surface varies with *ab initio* method is shown vividly in Fig. 2, which illustrates four principal surface types *a*, *b*, *c*, and *d* as exemplified by the DZ(d) CCSD, DZ(d) RHF, TZ(2d) CCSD(T), and TZ(2d) RHF cases, in order. It is astounding that each of the linear, L-shaped, and T-shaped structures is the global minimum of SiC_2 at some level of theory. Because the surface for pinwheel motion in this closed-shell molecule lies well below any dissociation threshold, symmetry considerations require the existence of both linear and T-shaped stationary points. The bent form exists whenever the adjacent linear structure is a minimum. In all cases it is a transition state connecting the linear form with L- or T-shaped triangular configurations. It is the existence of previously undocumented L-shaped minima in some theoretical computations which is problematic. Although there is overwhelming spectroscopic evidence that the carbon nuclei are equivalent in the $\tilde{X}\ ^1A_1$ state (*vide supra*), the question of whether the observed structure is in fact a vibrational average of identical L-shaped forms separated by a minuscule barrier has never been addressed or contemplated in the literature.

The perusal of the DZ(d) series starts with the observation that all correlation treatments with this basis set predict the linear form of SiC_2 to be a local minimum connected to triangular structures by a bent transition state lying 0.5–2.5 kcal mol^{-1} higher in energy. The reference [RHF, CASSCF(12,12)] bond lengths, r_e(C–C)=(1.2727, 1.3137) Å and r_e(Si–C)=(1.6756, 1.7179) Å, comprise intervals containing almost all of the dynamically correlated equilibrium distances, of which the CISD and MP4 values are the smallest and largest, respectively. The persistent oscillations

TABLE II. Total energies (hartree) of optimized SiC_2 structures.

Method	Linear	Bent	L-shaped	T-shaped
DZ(*d*) RHF	−364.498 551	−364.494 575	−364.494 670	−364.490 442
DZ(*d*) CASSCF(12,12)	−364.665 365	a	a	−364.661 080
DZ(*d*) MP2	−364.797 044	−364.795 461	b	−364.801 236
DZ(*d*) MP3	−364.808 704	−364.807 697	−364.811 779	−364.811 465
DZ(*d*) MP4	−364.840 959	−364.837 421	b	−364.838 367
DZ(*d*) MP5	−364.831 545	−364.830 596	b	−364.834 526
DZ(*d*) CISD	−364.782 953	−364.781 269	−364.784 168	−364.783 754
DZ(*d*) CISD+(Q)	−364.818 504	−364.817 146	−364.820 291	−364.820 551
DZ(*d*) CCSD	−364.816 124	−364.815 023	b	−364.818 732
DZ(*d*) CCSD(T)	−364.837 704	−364.836 112	b	−364.837 944
DZ(*d*) BD	−364.814 746	−364.813 708	−364.817 528	−364.817 515
DZ(*d*) BD(T)	−364.837 510	−364.835 972	b	−364.837 711
DZ(*d*) BD(TQ)	−364.836 209	−364.835 104	b	−364.838 225
TZ(2*d*) RHF	−364.507 707	b	−364.512 322	−364.507 866
TZ(2*d*) CISD	−364.820 516	b	−364.827 029	−364.826 206
TZ(2*d*) CISD+(Q)	−364.863 987	b	−364.867 678	−364.867 519
TZ(2*d*) CCSD	−364.859 142	b	−364.865 895	−364.865 775
TZ(2*d*) CCSD(T)	−364.884 972	a	−364.889 266	−364.889 287
TZ(2*d*1*f*) RHF	−364.514 135	−364.514 075	−364.517 295	−364.513 766
aug-cc-pVTZ CCSD(T)	−364.947 881	a	−364.953 595[c]	−364.953 976

[a]Optimization of this structure was not attempted (see the text).
[b]Not a stationary point at the given level of theory.
[c]Single-point energy at the TZ(2*d*) CCSD(T) geometry.

in the MP*n* distances are highlighted by the large MP4→MP5 contractions of about 0.02 Å. In ascending to the bent transition states, no bond length varies more than 0.004 Å. The angle of bending necessary to surmount the barrier is *broadly* correlated to the energy increase. Specifically, in the [MP4, RHF, CCSD(T), MP3, MP5] sequence, $\theta_e(\mathrm{Si–C–C})=(110.4°, 114.5°, 118.4°, 135.8°, 134.0°)$ while $E_{\mathrm{rel}}=(2.22, 2.50, 1.00, 0.63, 0.60)$ kcal mol^{-1}. The bending frequencies of 105–173 cm^{-1} for the linear form transform to 86*i*–119*i* cm^{-1} for the bent transition states. This geometric shift increases the Si–C stretching frequency predictions from the range 752–877 cm^{-1} to 923–1074 cm^{-1}. Finally,

TABLE III. Relative energies and harmonic vibrational frequencies of SiC_2 species.[a]

	$^1\Sigma^+$: Linear ($C_{\infty v}$)				$^1A'$: Bent (C_s)				$^1A'$: L-shaped (C_s)				$^1A_1$: T-shaped (C_{2v})			
Method	E_{rel}	$\omega_1(\sigma)$	$\omega_3(\sigma)$	$\omega_2(\pi)$	E_{rel}	ω_1	ω_2	ω_3	E_{rel}	ω_1	ω_2	ω_3	E_{rel}	$\omega_1(a_1)$	$\omega_2(a_1)$	$\omega_3(b_2)$
DZ(*d*) RHF	0.000	2055	877	173	2.495	1961	1074	95*i*	2.435	1938	1085	111	5.088	1976	851	328*i*
DZ(*d*) CASSCF(12,12)	0.000	1838	768	135		c				c			2.689	1730	801	221
DZ(*d*) MP2	0.000	1900	787	135	0.994	1821	923	119*i*		d			−2.630	1715	839	171
DZ(*d*) MP3	0.000	1987	834	117	0.632	1924	953	111*i*	−1.930	1818	956	160	−1.733	1846	850	135*i*
DZ(*d*) MP4	0.000	1779	752	145	2.219	1666	979	102*i*		d			1.626	1673	820	119
DZ(*d*) MP5	0.000	2003	826	108	0.596	1916	946	101*i*		d			−1.871	1805	836	73
DZ(*d*) CISD	0.000	1978	840	135	1.057	1903	987	115*i*	−0.762	1823	972	159	−0.503	1856	850	158*i*
					0.852[b]				−1.121[b]				−1.284[b]			
DZ(*d*) CCSD	0.000	1939	820	112	0.691	1862	957	98*i*		d			−1.636	1796	839	60
DZ(*d*) CCSD(T)	0.000	1875	786	111	0.999	1763	971	86*i*		d			−0.151	1745	823	123
DZ(*d*) BD	0.000	1950	824	114	0.651	1879	952	102*i*	−1.746	1793	883	95	−1.738	1802	843	61*i*
DZ(*d*) BD(T)	0.000	1879	787	112	0.965	1769	966	86*i*		d			−0.126	1744	823	113
DZ(*d*) BD(TQ)	0.000	1905	801	105	0.693	1808	952	86*i*		d			−1.265	1750	828	148
TZ(2*d*) RHF	0.000	2065	867	83*i*		d			−2.896	1929	1059	185	−0.100	1968	835	326*i*
TZ(2*d*) CISD	0.000	1980	829	100*i*		d			−4.086	1825	983	159	−3.570	1864	828	177*i*
									−2.316[b]				−2.217[b]			
TZ(2*d*) CCSD	0.000	1938	809	108*i*		d			−4.238	1778	910	107	−4.163	1805	814	91*i*
TZ(2*d*) CCSD(T)	0.000	1869	774	95*i*		c			−2.695	1714	902	51	−2.708	1747	796	57
TZ(2*d*1*f*) RHF	0.000	2059	873	56	0.038	2048	907	71*i*	−1.983	1928	1061	180	0.232	1972	839	299*i*
aug-cc-pVTZ CCSD(T)	0.000	1879	780	79*i*		c				d			−3.825	1751	798	137

[a]Relative energies (E_{rel}) in kcal mol^{-1}, harmonic vibrational frequencies (ω_i) in cm^{-1}.
[b]Davidson-corrected CISD relative energy.
[c]Optimization of these structures was not attempted.
[d]Not a stationary point at the given level of theory.

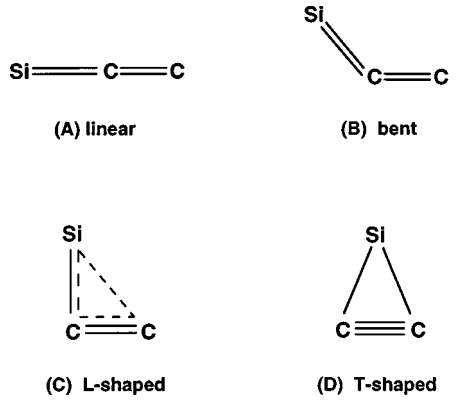

FIG. 1. Possible stationary points on the SiC_2 ground-state potential energy surface.

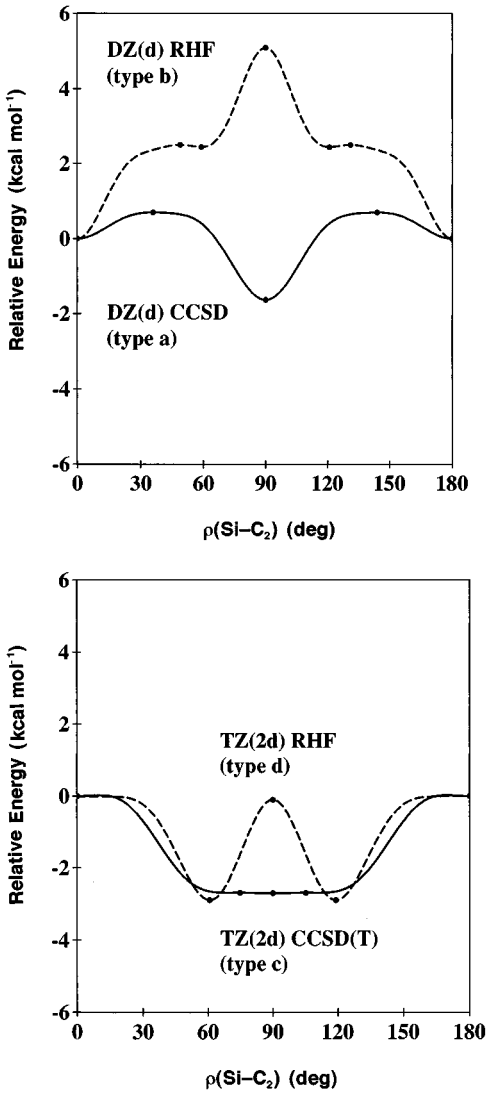

FIG. 2. Basic types of *ab initio* potential energy curves for pinwheel motion in SiC_2, as represented by the (a) DZ(d) CCSD, (b) DZ(d) RHF, (c) TZ(2d) CCSD(T), and (d) TZ(2d) RHF levels of theory. The abscissa is the Jacobi angle ρ(Si–C_2) between the C–C bond axis and the line connecting the midpoint of the C–C bond to the silicon spectator.

ω_1(C–C str.) exhibits large oscillations with level of theory in both the linear and bent stationary points, e.g., the MP4 and MP5 values for linear SiC_2 are 1779 and 2003 cm^{-1}, respectively. These oscillations are downshifted in position by 63–113 cm^{-1} in the bent *vis-à-vis* the linear form.

In the DZ(d) survey, it is remarkable that L-shaped structures exist in the RHF, MP3, CISD, and BD cases but not for the MP2, MP4, MP5, CCSD, CCSD(T), BD(T), and BD(TQ) methods. As illustrated in Fig. 2, the DZ(d) RHF minimum is merely a shallow, hanging well only 0.06 kcal mol^{-1} in depth on the downslope from the T-shaped transition state to the linear structure. In contrast, the L-shaped form in the MP3, CISD, and BD cases is the global SiC_2 minimum, lying below the linear and T-shaped stationary points by 0.76–1.93 and 0.008–0.26 kcal mol^{-1}, respectively. The minuscule energy differences between the L- and T-shaped forms are not to be associated with small variations in the geometric structures and vibrational frequencies, however. Among the L-shaped minima in the DZ(d) series, the r_e(Si–C) and θ_e(Si–C–C) predictions display ranges of 1.683–1.771 Å and 76.6°–102.1°, respectively, varying extensively with level of theory. In closing the ring, the Si–C separation increases to 1.834–1.837 Å and the Si–C–C angle diminishes to 69.35°–69.99°, suddenly both very narrow intervals. Mirroring the underlying geometric structures, the ω_2(Si–C str.) frequencies in the L form are substantially (40–234 cm^{-1}) higher than their ring counterparts. Finally, the bending frequencies of the L-shaped minima are comparable to the small $\omega_2(\pi)$ values of the linear configuration, but the order of analogous predictions for the two structures is sensitive to the correlation treatment.

The T-shaped structure of SiC_2 exhibits notable quirks in the DZ(d) series. In the RHF, MP3, CISD, and BD cases, it is a low-lying transition state for the interconversion of the aforementioned, equivalent L-shaped minima. At the CASSCF(12,12) and MP4 levels, it is a minimum lying 2.69 and 1.63 kcal mol^{-1}, respectively, above the preferred linear SiCC configuration. Nonetheless, the T-shaped structure is the global SiC_2 minimum in most instances, as demonstrated by a collection of (E_{rel}, ω_3) values in (kcal mol^{-1}, cm^{-1}) from Table III: MP2 [−2.630, 171], MP5 [−1.871, 73], CCSD [−1.636, 60], CCSD(T) [−0.151, 123], BD(T) [−0.126, 113], and BD(TQ) [−1.265, 148]. Relative to the linear configuration, the C–C bond length is contracted by 0.013±0.007 Å in the DZ(d) series, whereas the Si–C distance is increased by 0.139±0.008 Å (excluding the RHF case). Concomitantly, the C–C and Si–C stretching frequencies are shifted in the correlated computations by −152 ±46 cm^{-1} and +39±29 cm^{-1}, respectively, counterintuitive variations resulting from both kinetic and potential decoupling of these normal vibrations as the T-shaped configuration is adopted. As observed for the linear structure, the MPn predictions for r_e(C–C) and ω_1(C–C str.) vary widely in the T form, but the large oscillations are damped somewhat by the side-on electrostatic bonding of Si^+ to C_2^-. Meanwhile, the Si–C stretching frequency predictions are remarkably uniform, lying in the [820, 850] cm^{-1} interval

for all dynamically correlated DZ(d) computations.

The energetic data in Table III for the DZ(d) series highlight an overall stabilization due to electron correlation of triangular structures of SiC_2 over the linear form. The effect of double excitations is to drop $E_{\rm rel}$ from the RHF value of $+5.1$ kcal mol^{-1} to the (MP2, MP3) results of $(-2.6, -1.7)$ kcal mol^{-1}. Quadruple excitations provide additional stabilization of this type: the MP4(DQ) value of $E_{\rm rel}$ is -2.9 kcal mol^{-1}, and the BD(T)→BD(TQ) shift of this quantity is -1.1 kcal mol^{-1}. Nonetheless, the sizeable triples *destabilization* of triangular SiC_2 structures documented by previous workers[39–41] continues to be observed, as the DZ(d) MP4(SDQ)→MP4(SDTQ) and CCSD→CCSD(T) changes in $E_{\rm rel}$ are $-1.5\rightarrow+1.6$ and $-1.64\rightarrow-0.15$ kcal mol^{-1}, respectively.

The next step in the present methodological analysis of the SiC_2 polytopism problem focuses on the collection of TZ($2d$) and TZ($2d1f$) RHF, TZ($2d$) CISD, TZ($2d$) CCSD, and TZ($2d$) CCSD(T) results. When compared to analogous DZ(d) data, these results vividly demonstrate that basis set augmentation, particularly the addition of polarization functions, favors triangular configurations of SiC_2. In accord with ring-strain considerations, Grev and Schaefer[13] discovered such an effect in 1984, and the methodological study of Sadlej and co-workers[40] firmly established the phenomenon in 1988. The preferential lowering of triangular forms of SiC_2 is such that with the TZ($2d$) basis set, the linear structure becomes a transition state, the bent stationary point disappears, and the L form becomes a minimum (2–4 kcal mol^{-1} below linear) at all levels of theory employed here!

The larger triple-ζ basis sets expose a competition between the L- and T-shaped structures which is exceedingly intricate. The TZ($2d$) RHF relative energies of the (L,T) forms are $(-2.90, -0.10)$ kcal mol^{-1}, whereas further augmentation of the basis set with f functions yields $(-1.98, +0.23)$ kcal mol^{-1} predictions. Therefore, at the reference RHF level, larger basis sets appear to place the T form only slightly above or even below linear SiC_2, as previously observed,[40] but in these cases a very clear preference (>2 kcal mol^{-1}) is exhibited for the L-shaped structure over the T alternative. This initial preference is almost exactly canceled by successive correlation countereffects, as demonstrated by the following TZ($2d$) L–T energy differences: [RHF, CISD, CISD+(Q), CCSD, CCSD(T)]$=(-2.796, -0.516, -0.099, -0.075, +0.013)$ kcal mol^{-1}. The remarkable degree of cancellation within the higher-order correlation treatments leads to the strikingly flat TZ($2d$) CCSD(T) energy profile in Fig. 2. The harmonic vibrational analysis of the L and T stationary points given by the TZ($2d$) CCSD(T) method yields $\omega_3=51$ and 57 cm^{-1}, respectively, revealing *both* structures to be local minima. Presumably a tiny barrier on the order of 0.01 kcal mol^{-1} separates these minima, but our efforts to pinpoint this feature encountered persistent difficulties. In brief, at the TZ($2d$) CCSD(T) level of theory, the web of polytopism appears to have reached a fascinating extreme.

Notwithstanding the conspicuous variations in the bending potentials and associated vibrational frequencies provided by analogous DZ(d) and TZ($2d$) levels of theory, corresponding bond distances and stretching frequencies given by the two basis sets are in notable accord in the linear→L→T sequence of configurations. The trends in the r_e and ω_i data are the same in this sequence, and comparable DZ(d) and TZ($2d$) stretching frequencies vary only about 10 cm^{-1} on average. In particular, the TZ($2d$) ω(C–C) values first decrease by 152 cm^{-1} and then increase by 35 cm^{-1} in the mean, while r_e(C–C) contracts smoothly. Concomitantly, the TZ($2d$) ω(Si–C) values for the linear and T endpoints are comparable, lying 96–224 cm^{-1} lower than their L counterparts, whereas r_e(Si–C) expands smoothly over the interval. The change in r_e(Si–C) for the L→T transformation remains substantial in the TZ($2d$) predictions, the $+0.122$ Å average distortion serving to emphasize again that although the L and T forms are essentially isoenergetic, they occupy distinct geometric regions.

A resolution of the SiC_2 polytopism dilemma among the plethora of theoretical methods is afforded by aug-cc-pVTZ CCSD(T) searches of the pinwheel surface. Geometry optimizations at this level of theory starting from the TZ($2d$) CCSD(T) optimum L-shaped structure did not locate a minimum but simply led back to a triangular (C_{2v}) form. Energies computed along selected paths through the L-shaped region also indicate that there is no such aug-cc-pVTZ CCSD(T) minimum: these potential energy curves were found to decrease monotonically from starting points with obtuse Si–C–C angles through the anticipated L structure and onward to the T-shaped conformation. Moreover, the aug-cc-pVTZ CCSD(T) anharmonic force field for triangular (C_{2v}) SiC_2 (*vide infra*) was observed to not only closely reproduce the surface in the L region but also to exhibit no depressions in its contour maps of this area. As shown in Tables I and III, the final picture provided by the aug-cc-pVTZ CCSD(T) level of theory is that a linear transition state with [r_e(C–C), r_e(Si–C), $\omega_2(\pi)$]=(1.292 Å, 1.706 Å, $79i$ cm^{-1}) connects monotonically to a T-shaped global minimum with [r_e(C–C), r_e(Si–C), $\omega_3(b_2)$]=(1.280 Å, 1.853 Å, 137 cm^{-1}), which lies 3.82 kcal mol^{-1} lower in energy.

The key to the L-shaped vs T-shaped competition in SiC_2 appears to be unusually large contributions of higher-order polarization functions in extended correlation treatments of this system. This conclusion was tested here by computing additional energy points at the (linear, L, T) optimum structures given by the [aug-cc-pVTZ, TZ($2d$), aug-cc-pVTZ] CCSD(T) levels of theory, as documented in Tables II and IV. The CCSD(T) T-shaped/L-shaped energy difference of -0.24 kcal mol^{-1} with the aug-cc-pVTZ basis represents a significant stabilization of the T form over the TZ($2d$) value of -0.013 kcal mol^{-1}, owing to ($3d2f$) rather than ($2d$) polarization manifolds for each atom. Continued basis set augmentation to cc-pVQZ, whose atomic polarization scheme is ($3d2f1g$), more than doubles the CCSD(T) prediction of this quantity to -0.54 kcal mol^{-1}! In summary, there are both methodological and phenomenological reasons for concluding that the global minimum on

TABLE IV. Higher-level single-point energetic predictions for SiC_2 conformations.[a]

Method		Linear[b]		L-shaped[c]		T-shaped[b]	
		E_{total}	E_{rel}	E_{total}	E_{rel}	E_{total}	E_{rel}
cc-pVTZ	RHF	−364.531 653	0.000	−364.535 370	−2.332	−364.532 932	−0.803
	MP2	−364.898 236	0.000	−364.905 927	−4.826	−364.906 970	−5.481
cc-pVQZ	RHF	−364.539 450	0.000	−364.543 478	−2.528	−364.541 206	−1.102
	MP2	−364.929 383	0.000	−364.937 933	−5.365	−364.939 276	−6.208
	CCSD	−364.938 746	0.000	−364.947 781	−5.669	−364.948 445	−6.086
	CCSD(T)	−364.969 318	0.000	−364.975 734	−4.026	−364.976 590	−4.563
cc-pV5Z	RHF	−364.541 635	0.000	−364.545 723	−2.565	−364.543 483	−1.160
	MP2	−364.941 175	0.000	−364.950 235	−5.685	−364.951 682	−6.593
∞	RHF[d]	−364.542 486	0.000	−364.546 583	−2.571	−364.544 347	−1.17
	MP2[d]	−364.948 742	0.000	−364.958 403	−6.062	−364.959 928	−7.02

[a]Total energies in hartrees, relative energies in kcal mol^{-1}.
[b]aug-cc-pVTZ CCSD(T) geometry.
[c]TZ(2*d*) CCSD(T) geometry.
[d]Estimated total energies at the basis set limit (see the text). The ∞ MP2 entries are the sum of independently extrapolated RHF energies and second-order correlation corrections.

the SiC_2 surface is indeed a T-shaped equilibrium structure. In the end the L forms which exist at certain intermediate levels of theory gradually disappear as unusually high orders of polarization functions are included in extended correlation treatments.

Finally, the sensitivity of the SiC_2 electronic structure problem inescapably raises concern over multireference character in the ground-state electronic wave function. The Euclidian norm of the t_1 amplitudes given by the CCSD procedure is a common diagnostic for nondynamical electron correlation.[89] In the TZ(2*d*) and aug-cc-pVTZ coupled-cluster wave functions, this quantity is ca. 0.021 for the linear and T-shaped structures, or slightly higher than the suggested standard[89] of 0.020 for the onset of substantial multireference character. Nondynamical correlation of this magnitude should be recoverable with single-reference procedures as long as a contribution from connected triple excitations is present in the correlation treatment, as in the CCSD(T) method. The full valence DZ(*d*) CASSCF(12,12) method provides another important indicator. Representation of these multiconfigurational wave functions in terms of canonicalized, CASSCF natural orbitals reveals leading CI coefficients of (0.925, −0.127,−0.110) for linear and (0.930, −0.151, 0.107) for T-shaped conformations. Thus the reference configuration in the (linear, T-shaped) structures comprises (85.6%, 86.5%) of the total wave function, whereas the next two configurations additionally contribute only (2.8%, 3.4%). In brief, no competing configurations can be singled out, including the $(8a_1)^2 \rightarrow (4b_2)^2$ double excitation in the T-shaped system which describes diradical character in the strained, in-plane π bond of the C_2^- moiety. Finally, the near equivalence of analogous coupled-cluster and Brueckner predictions is indicative of limited nondynamical correlation in SiC_2. For example, the average difference in the (bond distances, stretching frequencies) in Tables I and III is (0.0011 Å, 7.5 cm^{-1}) for DZ(*d*) CCSD-BD and a mere (0.0002 Å, 2.8 cm^{-1}) for DZ(*d*) CCSD(T)-BD(T). These comparisons clearly demonstrate the sufficiency of RHF canonical orbitals rather than correlation-optimized Brueckner orbitals in higher-order treatments of SiC_2.

BARRIER TO LINEARITY AND HEAT OF FORMATION

Key thermochemical quantities of silicon dicarbide, such as the disputed barrier to linearity [Δ(T–L)] and the heat of formation, can be determined with increased reliability as a consequence of our completed methodological analysis of the polytopism problem. The Δ(T–L) difference predicted by the CCSD(T) method is −0.15, −2.71, −3.82, and −4.56 kcal mol^{-1} with the DZ(*d*), TZ(2*d*), aug-cc-pVTZ, and cc-pVQZ basis sets, in order. The continued stabilization of the T-shaped form in this series, even with the addition of atomic *g* functions, is remarkable. In contrast, the (T) correction to the CCSD energy not only favors the linear structure but is nearly invariant to basis set augmentation, the [DZ(*d*),TZ(2*d*), cc-pVQZ] contributions to Δ(T–L) being (1.48, 1.46, 1.52) kcal mol^{-1}. Finally, the DZ(*d*) BD(T) and BD(TQ) results reveal a sizeable (Q) increment in Δ(T–L) of −1.14 kcal mol^{-1}, which is likely to be insensitive to basis set given the behavior of the antecedent (T) correction. These pieces of data suggest that an explicit cc-pVQZ BD(TQ) value for Δ(T–L) would be close to $(-4.6)+(-1.1) = -5.7$ kcal mol^{-1}. In gauging the uncertainty of this result, it should be noted that continued basis set expansion should stabilize the T-shaped system further, whereas remaining high-order correlation terms might be expected to favor the linear structure, i.e., the oscillatory behavior of the correlation series suggests that BD(TQ) theory overshoots the true Δ(T–L) value.

A quantification of these effects and a final prediction for Δ(T–L) can be accomplished via extrapolations based on the additional cc-pVTZ through cc-pV5Z RHF and MP2 single-point energies presented in Table IV together with the application of Padé approximants to the DZ(*d*) MP2 through MP5 correlation energies. The correlation-consistent struc-

ture of the cc-pVnZ sets facilitates extrapolations of total energies to the one-particle basis set limit, because incremental energy lowerings fit approximate geometric series in the ζ parameter (n).[50] Specifically, by assuming a geometric ratio of $x=(\epsilon_5-\epsilon_4)(\epsilon_4-\epsilon_3)^{-1}$, the extrapolation

$$\epsilon_\infty=\epsilon_4+(\epsilon_5-\epsilon_4)(1+x+x^2+\cdots)$$
$$=\epsilon_4+\frac{\epsilon_5-\epsilon_4}{1-x}=\frac{\epsilon_4^2-\epsilon_3\epsilon_5}{2\epsilon_4-\epsilon_3-\epsilon_5},$$

has been employed here for ϵ_n equal to either the cc-pVnZ correlation energies or the corresponding RHF total energies, yielding the ∞ RHF and ∞ MP2 entries in Table IV. The continued stabilization of the T-shaped form of SiC_2 through the $(3d2f1g)\rightarrow(4d3f2g1h)$ augmentation and onward to the basis set limit is indisputable. In the Hartree–Fock limit, Δ(T–L) appears to lie near -1.2 kcal mol^{-1}, and the estimated MP2 counterpart is -7.0 kcal mol^{-1}. It is noteworthy that in the ∞ RHF case, L-shaped SiC_2 is actually the lowest-energy form, by 1.4 kcal mol^{-1}; however, the ∞ MP2 results place the T-shaped structure unambiguously below all others, consistent with the conclusions reached above. As inferred from the MP2 data in Table IV, the basis set incompleteness error for highly correlated cc-pVQZ predictions of Δ(T–L) is a sizeable 0.8 kcal mol^{-1}. To support the contention that in cc-pVQZ BD(TQ) computations this error would be mostly canceled by the inexactness of the electron correlation treatment, we have applied (shifted) [2,1] Padé approximants[90–92] to extrapolate the DZ(d) MPn correlation series to the full-CI limit at the linear and T-shaped MP5 optimum structures (Table I). Although not rigorous, the results give Δ(T–L)$=-0.58$ kcal mol^{-1}, suggesting that the corresponding BD(TQ) prediction is indeed 0.7 kcal mol^{-1} too large in magnitude. In other words, our error estimations provide a net shift of the previously surmised cc-pVQZ BD(TQ) energy difference of only $-0.8+0.7=-0.1$ kcal mol^{-1}. Accordingly, a final proposal of Δ(T–L)$=-5.8$ kcal mol^{-1} is advanced.

In comparison, the 1994 study of Ross *et al.*[33] performed stimulated emission pumping (SEP) of the $\tilde{X}\ ^1A_1/\tilde{A}\ ^1B_2$ system to locate $(0,0,v_3'')$ overtone levels and obtained a fitted SRB potential with an extrapolated barrier to linearity of 5.4 kcal mol^{-1}. As discussed in the introductory material, the spectroscopic data extended to Jacobi angles as small as 30° but were insufficient to give definitive features of the potential function any closer to linearity. Despite such limitations, the main conclusion is that agreement between theory and experiment on the salient aspects of the ground-state SiC_2 pinwheel surface has been now established, viz., the existence of a metastable linear isomer is ruled out; there is no depression on the surface which supports L-shaped minima; and the global minimum of SiC_2 is a T-shaped molecule lying 5–6 kcal mol^{-1} below the linear SiCC transition state.

The heat of formation of SiC_2 can be efficaciously investigated by means of the following reactions:

TABLE V. Gas-phase thermochemical data (kcal mol^{-1}) employed in the determination of $\Delta H_{f,0}^\circ$ of SiC_2.

Species	$\Delta H_{f,0}^\circ$[a]	ZPVE[b]
$C_2(^1\Sigma_g^+)$	198.2±0.9	2.64
$C_2(^3\Pi_u)$	200.2±0.9	2.34
Si(^3P)	106.66±1.9	···
$SiC_2(^1A_1)$	···	3.85

[a]Data from Ref. 93.
[b]The zero-point vibrational energies (ZPVEs) were evaluated using anharmonic molecular force fields. The data for C_2 are from Ref. 93, while the result for SiC_2 is from this work.

$$\text{Method A.}\quad \mathrm{Si}(^3P)+\mathrm{C_2}(\tilde{X}\ ^1\Sigma_g^+)\rightarrow \mathrm{SiC_2}(\tilde{X}\ ^1A_1), \tag{1}$$

$$\text{Method B.}\quad \mathrm{Si}(^3P)+\mathrm{C_2}(\tilde{a}\ ^3\Pi_u)\rightarrow \mathrm{SiC_2}(\tilde{X}\ ^1A_1). \tag{2}$$

The established thermochemical data listed in Table V provide $\Delta H_{f,0}^\circ(SiC_2)$ from accurate binding energies (ΔE_e) derived by the focal-point (fp) method of Allen and co-workers.[94–98] Here the fp scheme entails the primary computation of RHF, RCCSD, and RCCSD(T) total energies with the cc-pVDZ, cc-pVTZ, and cc-pVQZ basis sets accompanied by corrective cc-pVDZ UCCSD(T), UBD(T) and BD(TQ) results.[99] The total energies for all species in reactions (1) and (2) are collected in Table VI. Also provided in the table ($n.b.$ footnote b therein) are ∞ RHF, CCSD, and CCSD(T) estimates derived from a cc-pVnZ extrapolation scheme similar to that described above.

The focal-point analysis of ΔE_e for reactions (1) and (2) (Methods A and B) is laid out in Table VII. The validity of the fp method hinges on the rapid convergence of higher-order correlation *increments* for the reaction energy *vis-à-vis* basis set augmentation. This property is indeed actualized here. Note first that the cc-pVTZ→cc-pVQZ augmentation changes the leading correlation increment, δ[CCSD], by 3.04 and 3.17 kcal mol^{-1}, for ΔE_e of Methods A and B, respectively. However, these sizeable cc-pVTZ→cc-pVQZ shifts are followed by modifications of only 0.03 and 0.18 kcal mol^{-1} in the corresponding δ[CCSD(T)] contributions. Moreover, the extrapolation to an infinite basis predicts changes past cc-pVQZ for Methods A and B of 1.2–1.6 kcal mol^{-1} for δ[CCSD] but only 0.10–0.13 kcal mol^{-1} for δ[CCSD(T)]. The next correlation increment is taken from the cc-pVDZ UBD(TQ) computations, which reveal (Q) contributions of less than 1 kcal mol^{-1} for Methods A and B. Given the convergence behavior of the δ[CCSD(T)] term, it is justified to approximate δ[BD(TQ)] as the cc-pVDZ result throughout. In this way one arrives at the focal-point binding energies $\Delta E_e(1)=-152.14$ and $\Delta E_e(2)=-152.93$ kcal mol^{-1}. With the thermochemical data of Table V, these results then yield predictions of $\Delta H_{f,0}^\circ(SiC_2)=+153.9$ and $+155.4$ kcal mol^{-1} for Methods A and B, in order.

The residual errors in the reaction energies computed from the focal-point method include the neglect of valence correlation higher than fifth order in perturbation theory, as

TABLE VI. Total energies (hartree) of various species used in the determination of $\Delta H^{\circ}_{f,0}(SiC_2)$.[a]

Method	$C_2(^1\Sigma_g^+)$	$C_2(^3\Pi_u)$	$Si(^3P)$	$SiC_2(^1A_1)$
cc-pVDZ RHF	−75.386 902	−75.474 482	−288.846 421	−364.501 446
cc-pVDZ RCCSD	−75.699 129	−75.711 077	−288.913 953	−364.832 305
cc-pVDZ RCCSD(T)	−75.726 695	−75.724 242	−288.915 027	−364.851 694
cc-pVDZ UCCSD(T)	−75.726 695	−75.724 396	−288.915 089	⋯
cc-pVDZ UBD(T)	−75.725 229	−75.723 782	−288.920 192	−364.858 141
cc-pVDZ UBD(TQ)	−75.726 643	−75.726 130	−288.920 579	−364.858 641
cc-pVTZ RHF	−75.401 447	−75.488 602	−288.852 151	−364.532 932
cc-pVTZ RCCSD	−75.749 551	−75.762 109	−288.930 444	−364.921 332
cc-pVTZ RCCSD(T)	−75.783 070	−75.780 054	−288.933 032	−364.947 536
cc-pVQZ RHF	−75.405 765	−75.492 773	−288.854 107	−364.541 206
cc-pVQZ RCCSD	−75.765 696	−75.777 898	−288.934 559	−364.948 445
cc-pVQZ RCCSD(T)	−75.800 807	−75.797 113	−288.937 533	−364.976 590
∞ RHF[b]	−75.407 589	−75.494 522	−288.855 120	−364.544 156
∞ RCCSD[b]	−75.769 919	−75.782 589	−288.936 024	−364.956 707
∞ RCCSD(T)[b]	−75.805 468	−75.802 280	−288.939 139	−364.985 631

[a]For C_2, bond distances of 1.2425 Å ($^1\Sigma_g^+$) and 1.3119 Å ($^3\Pi_u$) were used (Ref. 93) while the aug-cc-pVTZ CCSD(T) geometry was employed for SiC_2. The C 1*s* and Si 1*s*, 2*s*, and 2*p* core orbitals were frozen in all computations except BD(T) and BD(TQ), in which only 1*s* cores were frozen due to orbital convergence problems encountered when the Si 2*s* and 2*p* sets were removed from the active space.

[b]These results are based on an extrapolation to the basis set limit by means of a geometric series, as described by Dunning (Ref. 50). The CCSD and CCSD(T) total energies were estimated by fitting to a geometric series the incremental correlation energy lowerings in the cc-pV*n*Z sequence ($n=1, 2, 3, 4$) and adding the predicted higher-order ($n>4$) contributions to the correlation energy obtained with the cc-pVQZ set. The ∞ RHF energies were obtained in a similar way by fitting RHF energy lowerings to a geometric series.

well as core and core–valence correlation. Of course, the basis-set extrapolation scheme, which increases the binding energies by 1.4–1.8 kcal mol^{-1}, is also inexact. The recovery of valence electron correlation in Method A is expected to be more problematic than in Method B, because the $C_2(\tilde{X}\ ^1\Sigma_g^+)$ fragment has a substantial contribution in the ground-state wave function arising from the $(3\sigma_g)^2 \rightarrow (2\sigma_u)^2$ excitation. This nondynamical correlation effect appears to be manifested in the larger δ[CCSD(T)] and δ [BD(TQ)] increments for reaction (1). In fact, the aforementioned $\|t_1\|$ diagnostic[89] is about 0.021 for SiC_2, Si, and $C_2(^3\Pi_u)$, but ca. 0.038 for $C_2(^1\Sigma_g^+)$, substantiating the considerable multireference character of the singlet C_2 species. Therefore, one might be inclined to ascribe more weight to

TABLE VII. Evaluation of $\Delta H^{\circ}_{f,0}(SiC_2)$ by Methods A and B.[a]

	cc-pVDZ	cc-pVTZ	cc-pVQZ	∞[b]
A. $Si(^3P)+C_2(\tilde{X}\ ^1\Sigma_g^+)\rightarrow SiC_2(\tilde{X}\ ^1A_1)$				
ΔE_e[RHF]	−168.25	−175.28	−176.54	−176.61
δ[RCCSD]	+30.68	+23.84	+20.80	+19.26
δ[RCCSD(T)]	+5.80	+6.21	+6.24	+6.11
δ[UBD(TQ)]	−0.90	[−0.90]	[−0.90]	[−0.90]
ΔE_e(corr)	−132.67	[−146.13]	[−150.40]	[−152.14]
$\Delta E_0 = \Delta E_e$[fp] + Δ[ZPVE]$=-152.14+1.21$ kcal mol^{-1} $= -150.93$ kcal mol^{-1}				
$\Delta H^{\circ}_{f,0}(SiC_2) = \Delta E_0 + \Delta H^{\circ}_{f,0}(Si) + \Delta H^{\circ}_{f,0}[C_2(\tilde{X}\ ^1\Sigma_g^+)]$ $= -150.93+106.66+198.2=$ **153.9** kcal mol^{-1}				
B. $Si(^3P)+C_2(\tilde{a}\ ^3\Pi_u)\rightarrow SiC_2(\tilde{X}\ ^1A_1)$				
ΔE_e[RHF]	−113.29	−120.59	−121.94	−122.06
δ[RCCSD]	−16.78	−22.97	−26.14	−27.34
δ[RCCSD(T)]	−3.23	−3.56	−3.74	−3.84
δ[UBD(TQ)]	+0.31	[+0.31]	[+0.31]	[+0.31]
ΔE_e(corr)	−132.99	[−146.81]	[−151.51]	[−152.93]
$\Delta E_0 = \Delta E_e$[fp]+Δ[ZPVE]$=-152.93+1.51=-151.42$ kcal mol^{-1}				
$\Delta H^{\circ}_{f,0}(SiC_2) = \Delta E_0 + \Delta H^{\circ}_{f,0}(Si) + \Delta H^{\circ}_{f,0}[C_2(\tilde{a}\ ^3\Pi_u)]$ $= -151.42+106.66+200.2=$ **155.4** kcal mol^{-1}				

[a]All entries in kcal mol^{-1}. In the focal-point (fp) extrapolations of correlation (corr) series, the symbol δ denotes the *increment* in the reaction energy (ΔE_e) relative to the preceding level of theory. The increments in brackets are assumed values based on the cc-pVDZ BD(TQ) prediction.

[b]Derived from total energies extrapolated to an infinite basis set, as described in footnote b of Table VI.

TABLE VIII. Complete aug-cc-pVTZ CCSD(T) quartic force field of SiC_2.[a]

ij	F_{ij}	ijk	F_{ijk}	$ijkl$	F_{ijkl}
Valence internal coordinates: $\{S_1=r(\mathrm{C–C}),\ S_2=2^{-1/2}[r_1(\mathrm{Si–C})+r_2(\mathrm{Si–C})],\ S_3=2^{-1/2}[r_1(\mathrm{Si–C})-r_2(\mathrm{Si–C})]\}$					
11	10.995	111	−67.44	1111	336.7
21	−0.6526	211	0.715	2111	1.62
22	2.7527	221	0.991	2211	−2.22
33	0.1208	222	−9.293	2221	−2.53
		331	−1.491	2222	27.28
		332	−8.963	3311	1.01
				3321	0.47
				3322	28.15
				3333	76.13
Jacobi internal coordinates: $\{S_1=r(\mathrm{C–C}),\ S_2=R(\mathrm{Si–C_2}),\ S_3=\rho(\mathrm{Si–C_2})\}$					
11	10.840	111	−66.86	1111	338.3
21	0.0258	211	1.465	2111	−1.52
22	4.8492	221	−3.152	2211	−5.39
33	0.08711	222	−20.73	2221	16.44
		331	−2.539	2222	73.76
		332	−9.575	3311	−6.56
				3321	−5.04
				3322	37.99
				3333	50.67

[a]The units of the force constants are consistent with energy in aJ, distances in Å, and angles in rad.

the (higher) Method B result for $\Delta H^{\circ}_{f,0}(SiC_2)$, and thus we advance a value of $\Delta H^{\circ}_{f,0}(SiC_2)=155\pm3$ kcal mol^{-1}.

The accepted value[93] for $\Delta H^{\circ}_{f,0}(SiC_2)$, which is 145.6 ±6.9 kcal mol^{-1}, is based on pre-1965 mass spectrometric studies of vapor-phase equilibria over the systems SiC–graphite, SiC–silicon, and boron–carbon–silicon. Our proposal represents a substantial revision of this empirical heat of formation and a large reduction of the associated uncertainty. The error intervals of the experimental and theoretical values barely overlap, calling for renewed laboratory work to investigate the disparity. The most notable competing theoretical value for $\Delta H^{\circ}_{f,0}(SiC_2)$ is 150.9 kcal mol^{-1}, obtained via the G2 method in the aforementioned study of Deutsch and Curtiss.[41] The G2 method[42] employs additivity approximations to obtain effective QCISD(T)/6-311+G($3df$,$2p$) total energies, to which an empirical higher level correction (HLC) is appended. Notwithstanding the systematic calibration studies bolstering the G2 method and the HLC in particular, the current focal-point analysis entails direct computations and extrapolations which are more complete both in terms of the one-particle basis set and the correlation treatment. The 4 kcal mol^{-1} difference in the competing theoretical predictions may arise from unusually severe basis set requirements of the SiC_2 system, as suggested by the large effect that atomic g functions have on the pinwheel surface. In this regard it is noteworthy that the G2 prediction for Δ(T–L) of SiC_2 is -3.51 kcal mol^{-1}, which is 2.2 kcal mol^{-1} smaller in magnitude than the barrier to linearity surmised here. In brief, the current prediction, $\Delta H^{\circ}_{f,0}(SiC_2)=155\pm3$ kcal mol^{-1}, should be considered the best value among available theoretical and experimental results.

ANHARMONIC FORCE FIELD

Definitive studies of the unusual rovibrational dynamics of SiC_2 will require analytic representations of the polytopic potential energy surface. However, a preliminary representation of the anharmonic surface in the region of the T-shaped equilibrium geometry is provided by the complete quartic force fields specified in Table VIII. Force constants determined at the aug-cc-pVTZ CCSD(T) level of theory are listed therein in two internal coordinate systems: (1) a standard valence set of (symmetrized) bond distances, and (2) the Si–C_2 Jacobi variables involving the distance (R) and angle (ρ) of the silicon spectator with respect to the midpoint of the C_2 fragment. The Jacobi coordinates provide a more natural description of T-shaped molecules executing large-amplitude pinwheel motion. In particular, the F_{21} quadratic coupling constant is much smaller in the Jacobi representation than in the standard valence coordinate set, consistent with the anticipated structure[18] of the normal modes of a T-shaped species exhibiting nondirectional bonding. Nonetheless, the two force fields provide contour plots for large-amplitude motion which are hardly distinguishable. In Fig. 3 comparative contours for silicon excursions about a fixed C_2 moiety are shown, as given by the quadratic (top) and then quartic (bottom) force fields in the valence internal coordinate representation. Three features of the plots are salient: (1) there are no depressions in the contours arising from an L-shaped mini-

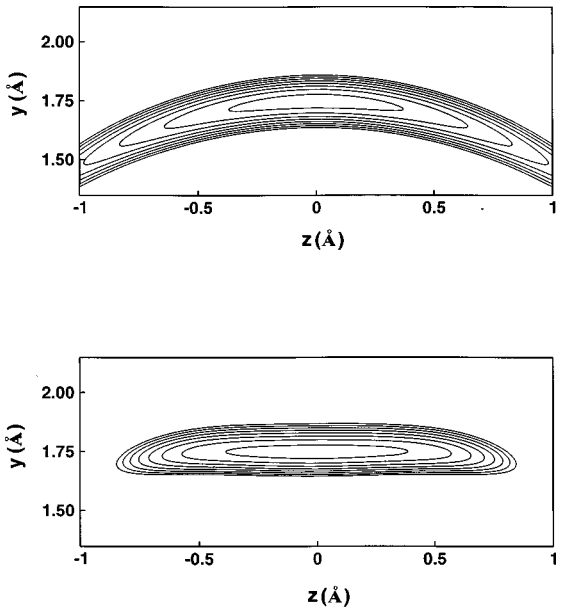

FIG. 3. Contour plots of the aug-cc-pVTZ CCSD(T) quadratic (top) and quartic (bottom) force fields of SiC_2 from the valence internal coordinate representation. The Cartesian plots correspond to the motion of silicon in the yz plane about a fixed C_2 moiety lying along the z axis. Contours are drawn every 200 cm^{-1}, beginning at 100 cm^{-1} above the T-shaped SiC_2 minimum.

mum or any related artifact of the electronic structure problem; (2) the effect of the anharmonic terms in the force field is to *straighten out* the trough for pinwheel excursions; and (3) the vibrational amplitudes occurring in the low-energy pinwheel eigenstates are extreme. In brief, the anharmonic force field yields a surface which favors *rectilinear* vibrations of silicon parallel to the axis of C_2 fully spanning a 1 Å range within the first 1 kcal mol^{-1} of energy! This remarkable behavior is indeed polytopic in character. Limitations of force field representations of the surface are thus expected. Of course, further extension of the contours of the anharmonic force field does eventually redirect the trough through linear SiCC configurations, restoring curvilinearity to the path for higher-energy pinwheel motion.

Some efforts were made to test the validity of the quartic force field representation from which the bottom contour plot in Fig. 3 was generated. Single-point aug-cc-pVTZ CCSD(T) energies were computed at 16 locations obtained by displacing normal coordinates, individually as well as collectively, around the minimum, and these energies were compared to those predicted by the force field. The test geometries included displacements of one or two normal coordinates just beyond the classical points of the fundamental (ν_1,ν_2,ν_3) vibrational levels, and all displacements involved bond-length distortions greater than or equal to 0.06 Å. The differences between the actual aug-cc-pVTZ CCSD(T) energies and those predicted by the quartic force field were less than 15 cm^{-1} in all cases except one, where the difference was 36 cm^{-1}. By adjusting the F_{111}, F_{1111}, F_{331}, F_{3311}, F_{332}, F_{3322}, and F_{3321} force constants to fit the test energy points to less than 5 cm^{-1} in all cases, anharmonic fundamental vibrational frequencies were obtained by second-order perturbation theory[100] which differed from the original values by less than 7 cm^{-1}. Therefore, it appears that quartic force fields provide a representation of the anharmonic surface which is adequate at least for a preliminary exploration of the low-lying vibrational eigenstates of SiC_2.

TABLE IX. Anharmonic constants (χ_{ij}) and harmonic vibrational frequencies (ω_i) of SiC_2 predicted by the aug-cc-pVTZ CCSD(T) level of theory.[a]

$\omega_1(a_1)=1751$	$\omega_2(a_1)=798$	$\omega_3(b_2)=137$
$\chi_{11}=-11.34$	$\chi_{21}=-1.70$	$\chi_{31}=-23.49$
$\chi_{22}=-2.73$	$\chi_{32}=85.60$	$\chi_{33}=-32.10$

[a]All quantities in cm^{-1}.

The 1991 dispersed fluorescence (DF) study of Butenhoff and Rohlfing[32] yielded 43 vibrational term energies of the SiC_2 ground state involving long progressions in the ν_3 mode. These progressions exhibit extreme negative anharmonicity and periodic resonances arising from strong coupling between ν_2 and ν_3 vibrations. The variation of the energy levels with respect to the quantum numbers for C–C and Si–C_2 stretching is reasonably reckoned by the standard spectroscopic constants $\omega_1=1756.8$, $\omega_2=844.0$, $\chi_{11}=-11.8$, $\chi_{22}=-4.58$, and $\chi_{21}=-3.8$ cm^{-1}, but the extensive ν_3 progressions cannot be accounted for by second-order perturbation theory.

Similar conclusions are reached on the basis of the anharmonic constants reported in Table IX, which are derived from the aug-cc-pVTZ CCSD(T) quartic force field. The agreement between theory and experiment for ω_1 and χ_{11} is indeed quantitative (6 and 0.5 cm^{-1} errors, respectively). The Si–C_2 stretching frequency is underestimated by 46 cm^{-1}, indicative of a predicted bond which is not tight enough (*vide infra*), and the theoretical χ_{22} and χ_{21} anharmonic terms appear to be too small in magnitude as well. Nonetheless, the level of accord is within reason. Considerable difficulties are encountered in all parameters involving the pinwheel mode ν_3, however. First, the aug-cc-pVTZ CCSD(T) result for ω_3 is 137 cm^{-1}, with a total predicted anharmonicity of -33 cm^{-1}. In view of the established[32,33] empirical fundamental, $\nu_3=196.37$ cm^{-1}, the theoretical harmonic frequency must be too small by a factor greater than 1.5. Second, *effective* anharmonic constants for the ν_3 mode can be extracted from the lowest-lying fundamental, overtone, and combination levels tabulated by Butenhoff and Rohlfing.[32,33] These empirical quantities are

$$\chi_{32}=(\nu_2+\nu_3)-\nu_2-\nu_3$$
$$=1072.2-840.6-196.4=35.2\ \ cm^{-1},$$

$$\chi_{31}=(\nu_1+\nu_3)-\nu_1-\nu_3$$
$$=1925-1746-196=-17\ \ cm^{-1},$$

and

$$\chi_{33}=(1/2)(2\nu_3)-\nu_3$$
$$=(1/2)(352.8)-196.4=-19.9\ \ cm^{-1}.$$

TABLE X. Vibration–rotation interaction constants (α_i, 10^{-3} cm^{-1}) for SiC_2 isotopomers predicted by the aug-cc-pVTZ CCSD(T) force field.

	$^{28}SiC_2$	$^{28}Si^{12}C^{13}C$	$^{29}SiC_2$	$^{30}SiC_2$
α_1^A	−36.61	−34.49	−36.61	−36.61
α_2^A	−1.23	−0.70	−1.22	−1.22
α_3^A	24.22	22.60	24.40	24.57
α_1^B	−0.26	−0.26	−0.26	−0.26
α_2^B	2.06	1.88	2.01	1.97
α_3^B	14.80	14.19	14.55	14.32
α_1^C	−1.65	−1.60	−1.61	−1.57
α_2^C	1.26	1.15	1.24	1.22
α_3^C	12.23	11.69	12.08	11.93

The corresponding theoretical anharmonic constants from Table IX are all much larger in magnitude than these effective values, particularly in the extreme $\chi_{32}=85.60$ cm^{-1} case. Finally, the overestimation of the χ_{32} constant engenders a highly dubious total anharmonicity prediction (+36 cm^{-1}) for the Si–C_2 stretching mode.

In summary, an instructive view of the SiC_2 surface is provided by the aug-cc-pVTZ CCSD(T) quartic force field. The trough containing the T-shaped minimum favors low-energy *rectilinear* motion of extreme amplitude for silicon excursions parallel to the C_2 axis. An expansion of the potential energy function through fourth order appears to provide an acceptable representation for the description of the *lowest* eigenstates for this motion, but the application of spectroscopic perturbation theory to this problem is fraught with difficulties. Moreover, while the aug-cc-pVTZ CCSD(T) level of theory correctly predicts the basic features of the SiC_2 polytopism problem, it is still insufficient to obtain quantitative information for the ν_3 vibrational levels. Future work on these vibrations should employ an electronic structure method which gives a larger separation (>5 kcal mol^{-1}) for Δ(T–L) and an attendant ν_3 potential function with greater curvature.

EQUILIBRIUM (R_e) STRUCTURE OF SiC_2

The anharmonic force field determined at the aug-cc-pVTZ CCSD(T) level of theory can also be employed in a preliminary investigation of zero-point vibrational effects on the molecular structure of SiC_2. The empirical rotational constants from the voluminous high-resolution rotational spectroscopic work[14–16,21–30] reviewed above can be interfaced with theoretical vibration–rotation interaction constants (α_i) to determine equilibrium (r_e) structural parameters. Bogey and co-workers[27] have compiled high-resolution rotational constants (A_0,B_0,C_0) for $^{28}SiC_2$, $^{29}SiC_2$, $^{30}SiC_2$, and $^{28}Si^{13}C^{12}C$, and the aug-cc-pVTZ CCSD(T) α_i constants for these isotopomers are listed in Table X. Each (A_0,B_0,C_0) set exhibits a pronounced inertial defect near 0.35 u $Å^2$. For T-shaped SiC_2 isotopomers with equivalent carbon atoms, the carbon–carbon bond length directly determines the a-axis moment of inertia (I_a). Likewise, the b-axis moment (I_b) is governed by the distance of silicon to the midpoint of the C–C bond. In view of the large inertial defect, it is thus preferable to ascertain the molecular structure from the (A_0,B_0) sets alone. Assuming equal weights for all isotopomeric data in a least-squares refinement, we then obtain r_0(C–C)=1.2670(2) Å and r_0(Si–C)=1.8369(1) Å, essentially the same parameters reported by Thaddeus *et al.*[14] If the zero-point vibrational contributions are deflated from the (A_0,B_0,C_0) isotopomeric data sets by means of the theoretical α_i constants, then the inertial defect is reduced in all cases, but only to about 0.21 u $Å^2$.[101] Our least-squares refinement procedure yields r_e(C–C)=1.2694(3) Å and r_e(Si–C)=1.8222(1) Å from the resulting (A_e,B_e) estimates. The direct algebraic solutions for these distances given by the $^{28}SiC_2$ rotational constants alone are identical within 0.0001 Å, revealing the consistency of the isotopomeric (A_e,B_e) pairs. These carbon-carbon and silicon-carbon bond lengths are 0.0009 Å larger and 0.010 Å smaller, in order, than those present in the substitution (r_s) structure extracted from the same empirical rotational constants by Bogey and co-workers.[27]

The r_e-r_0 differences resulting from the least-squares analysis are +0.0025 Å and −0.0147 Å for the C–C and Si–C bonds, respectively. The zero-point vibrational shift of the carbon-carbon distance toward smaller effective values is, of course, peculiar, if not dubious. It is noteworthy that the published r_s(C–C) parameter[27] is also longer than its r_0 counterpart. Such unusual behavior may actually be a physical manifestation of large-amplitude motion in the ν_3 mode, but this point is clouded by the considerable inertial defect remaining in the empirically based (A_e,B_e,C_e) estimates. Specifically, if the complete (A_0,B_0,C_0) and (A_e,B_e,C_e) data sets are employed in our least-squares procedure, i.e., the c-axis inertial moments are also included, then the results are [r_0(C–C), r_0(Si–C)] =[1.275(3), 1.8406(9)] Å and [r_e(C–C), r_e(Si–C)] =[1.274(2), 1.8245(6)] Å. In brief, alternate C–C distances are obtained which are over 0.005 Å larger than before and which do not exhibit the peculiar r_e-r_0 shift.

The validity of the empirically based r_e results can be gauged by more detailed *ab initio* considerations of the SiC_2 equilibrium structure. The aug-cc-pVTZ CCSD(T) predictions of [r_e(C–C), r_e(Si–C)]=(1.2798, 1.8534) Å provide a convenient reference geometry. Because the CCSD→CCSD(T) changes in the bond lengths depend only weakly on the one-particle basis (Table I), it is reasonable to adopt the DZ(d) BD(T)→BD(TQ) [δr(C–C), δr(Si–C)] shifts of (−0.0006, −0.0019) Å as corrections due to higher-order electron correlation effects. The consequences of basis set incompleteness can be estimated as the aug-cc-pVTZ→aug-cc-pVQZ CCSD(T) contractions in the ground-state equilibrium bond distances of $C_2(^1\Sigma_g^+)$ and $SiC(^1\Sigma^+)$, viz., 0.0049 Å (1.2509→1.2460 Å) and 0.0107 Å (1.8374→1.8267 Å). Finally, our calibrations[102] suggest shifts in the bond distances due to core correlation of −0.0031 and −0.0044 Å, in accord with other studies.[103–106] The composite *ab initio* predictions for the T-shaped structure of SiC_2 are thus r_e(C–C)=1.2798−0.0006−0.0049 −0.0031=1.2712 Å and r_e(Si–C)=1.8534−0.0019 −0.0107−0.0044=1.8364 Å. The same scheme applied to

diatomic $C_2(^1\Sigma_g^+)$ yields $r_e = 1.2423$ Å, which is in exceptional agreement with the spectroscopic equilibrium length (1.2425 Å).[20] Therefore, the *ab initio* evidence suggests that the bond distances in SiC_2 are underestimated from the fit to the (A_e, B_e) estimates alone. While r_e(C–C) seems to be pinpointed at 1.271 ± 0.003 Å, a discrepancy greater than 0.01 Å between theory and experiment remains to be resolved for r_e(Si–C).

CONCLUDING REMARKS

In the Prospectus of this paper the goals of this study were set forth, and key results are summarized in the Abstract. An extensive methodological analysis has been completed in order to resolve the polytopism problem of the $Si–C_2$ pinwheel surface; high-level thermochemical predictions have been advanced for the barrier to linearity, the $Si–C_2$ binding energy, and hence the heat of formation of silicon dicarbide; and a complete quartic force field has been determined in a preliminary investigation of the surface for large-amplitude motion, aspects of the vibrational anharmonicity, and the equilibrium molecular structure. Consequently, the challenge to *ab initio* theory presented by the SiC_2 molecule has been firmly documented, elevating this species as a testing ground for methodological development. A quantitative mapping of the SiC_2 surface will require a level of theory commensurate with cc-pVQZ BD(TQ), because both *g* polarization manifolds in the atomic-orbital basis and correlation corrections for connected quadruple excitations are necessary to correctly obtain the Δ(T–L) separation and the $\omega_3(b_2)$ harmonic frequency. The complete *ab initio* recovery and/or confirmation of the proliferation of definitive spectroscopy on this system will undoubtedly persist for some time.

ACKNOWLEDGMENTS

The authors would like to thank Dr. Timothy J. Lee, Dr. Celeste M. Rohlfing, and Dr. Marcel Bogey for helpful discussions on the SiC_2 problem. Part of this work was funded by Sandia National Laboratories under contract from the U. S. Department of Energy and supported by its Division of Basic Energy Sciences. The work of A. G. Császár is supported by the Scientific Research Foundation of Hungary (OTKA T024044).

[1] P. W. Merrill, Publ. Astron. Soc. Pac. **38**, 175 (1926).
[2] R. F. Sanford, Publ. Astron. Soc. Pac. **38**, 177 (1926).
[3] A. McKellar, J. R. Astron. Soc. Can. **41**, 147 (1947).
[4] R. F. Sanford, Astrophys. J. **111**, 262 (1950).
[5] B. Kleman, Astrophys. J. **123**, 162 (1956).
[6] J. Drowart, G. De Maria, and M. G. Inghram, J. Chem. Phys. **29**, 1015 (1958).
[7] W. Weltner and D. McLeod, J. Chem. Phys. **41**, 235 (1964).
[8] R. D. Verma and S. Nagaraj, Can. J. Phys. **52**, 1938 (1974).
[9] V. E. Bondybey, J. Phys. Chem. **86**, 3396 (1982).
[10] E. A. Rohlfing, J. Chem. Phys. **91**, 4531 (1989).
[11] S. Green, Astrophys. J. **266**, 895 (1983).
[12] D. L. Michalopoulos, M. E. Geusic, P. R. R. Langridge-Smith, and R. E. Smalley, J. Chem. Phys. **80**, 3556 (1984).
[13] R. S. Grev and H. F. Schaefer, J. Chem. Phys. **80**, 3552 (1984).
[14] P. Thaddeus, S. E. Cummins, and R. A. Linke, Astrophys. J. **283**, L45 (1984).
[15] L. E. Snyder, C. Henkel, J. M. Hollis, and F. J. Lovas, Astrophys. J. **290**, L29 (1985).
[16] J. Cernicharo, C. Kahane, J. Gómez-González, and M. Guélin, Astron. Astrophys. **167**, L9 (1986).
[17] R. A. Shepherd and W. R. M. Graham, J. Chem. Phys. **82**, 4788 (1985).
[18] R. A. Shepherd and W. R. M. Graham, J. Chem. Phys. **88**, 3399 (1988).
[19] J. D. Presilla-Márquez, W. R. M. Graham, and R. A. Shepherd, J. Chem. Phys. **93**, 5424 (1990).
[20] K. P. Huber and G. Herzberg, *Constants of Diatomic Molecules* (Van Nostrand Reinhold, New York, 1979).
[21] H. Bredohl, I. Dubois, H. Leclercq, and F. Mélen, J. Mol. Spectrosc. **128**, 399 (1988).
[22] C. A. Gottlieb, J. M. Vrtílek, and P. Thaddeus, Astrophys. J. **343**, L29 (1989).
[23] J. Cernicharo, C. A. Gottlieb, M. Guélin, P. Thaddeus, and J. M. Vrtílek, Astrophys. J. **341**, L25 (1989).
[24] R. D. Suenram, F. J. Lovas, and K. Matsumura, Astrophys. J. **342**, L103 (1989).
[25] J. Cernicharo, M. Guélin, C. Kahane, M. Bogey, C. Demuynck, and J. L. Destombes, Astron. Astrophys. **246**, 213 (1991).
[26] M. Bogey, C. Demuynck, D. L. Destombes, and A. D. Walters, Astron. Astrophys. **247**, L13 (1991).
[27] M. Bogey, M. Cordonnier, C. Demuynck, and J. L. Destombes, in *Structures and Conformations of Non-Rigid Molecules*, edited by J. Laane, M. Dakkouri, B. van der Veken, and H. Oberhammer (Kluwer, Dordrecht, 1993), p. 303.
[28] L. H. Coudert, J. Mol. Spectrosc. **160**, 225 (1993).
[29] S. Chandra and A. Sahu, Astron. Astrophys. **272**, 700 (1993).
[30] M. Izuha, S. Yamamoto, and S. Saito, Spectrochim. Acta A **50**, 1371 (1994).
[31] R. Fantoni, F. Bijnen, N. Djurić, and S. Piccirillo, Appl. Phys. B **52**, 176 (1991).
[32] T. J. Butenhoff and E. A. Rohlfing, J. Chem. Phys. **95**, 1 (1991).
[33] S. C. Ross, T. J. Butenhoff, E. A. Rohlfing, and C. M. Rohlfing, J. Chem. Phys. **100**, 4110 (1994).
[34] P. R. Bunker and B. M. Landsberg, J. Mol. Spectrosc. **67**, 374 (1977); P. R. Bunker, Annu. Rev. Phys. Chem. **34**, 59 (1983); P. Jensen, Comput. Phys. Rep. **1**, 1 (1983).
[35] F. Pauzat and Y. Ellinger, Chem. Phys. Lett. **112**, 519 (1984).
[36] J. Oddershede, J. R. Sabin, G. H. F. Diercksen, and N. E. Grüner, J. Chem. Phys. **83**, 1702 (1985).
[37] E. Clementi, H. Kistenmacher, and H. Popkie, J. Chem. Phys. **58**, 2460 (1973).
[38] T. Törring, J. P. Bekooy, W. L. Meerts, J. Hoeft, E. Tiemann, and A. Dymanus, J. Chem. Phys. **73**, 4875 (1980).
[39] G. Fitzgerald, S. J. Cole, and R. J. Bartlett, J. Chem. Phys. **85**, 1701 (1986).
[40] A. J. Sadlej, G. H. F. Diercksen, J. Oddershede, and J. R. Sabin, Chem. Phys. **122**, 297 (1988).
[41] P. W. Deutsch and L. A. Curtiss, Chem. Phys. Lett. **226**, 387 (1994).
[42] L. A. Curtiss, K. Raghavachari, G. W. Trucks, and J. A. Pople, J. Chem. Phys. **94**, 7221 (1991).
[43] L. A. Curtiss, J. E. Carpenter, K. Raghavachari, and J. A. Pople, J. Chem. Phys. **96**, 9030 (1992); L. A. Curtiss, K. Raghavachari, and J. A. Pople, *ibid.* **98**, 1293 (1993).
[44] S. Arulmozhiraja and P. Kolandaivel, J. Mol. Struct. (Theochem) **334**, 71 (1995).
[45] R. S. Grev and H. F. Schaefer, J. Am. Chem. Soc. **111**, 5687 (1989).
[46] S. Huzinaga, J. Chem. Phys. **42**, 1293 (1965).
[47] T. H. Dunning, Jr., J. Chem. Phys. **53**, 2823 (1970).
[48] T. H. Dunning, Jr. and P. J. Hay, in *Modern Theoretical Chemistry*, edited by H. F. Schaefer (Plenum, New York, 1977), Vol. 3, p. 24.
[49] E. Magnusson, J. Comput. Chem. **14**, 54 (1993).
[50] T. H. Dunning, Jr., J. Chem. Phys. **90**, 1007 (1989).
[51] D. E. Woon and T. H. Dunning, Jr., J. Chem. Phys. **98**, 1358 (1993).
[52] R. A. Kendall, T. H. Dunning, Jr., and R. J. Harrison, J. Chem. Phys. **96**, 6796 (1992).
[53] C. C. J. Roothaan, Rev. Mod. Phys. **23**, 69 (1951).
[54] W. J. Hehre, L. Radom, P. v. R. Schleyer, and J. A. Pople, *Ab Initio Molecular Orbital Theory* (Wiley-Interscience, New York, 1986).

[55] A. Szabo and N. S. Ostlund, *Modern Quantum Chemistry*, 1st edition, revised (McGraw-Hill, New York, 1989).
[56] B. O. Roos, in *Ab Initio Methods in Quantum Chemistry*, edited by K. P. Lawley (Wiley, New York, 1987), p. 399.
[57] C. Møller and M. S. Plesset, Phys. Rev. **46**, 618 (1934).
[58] J. A. Pople, J. S. Binkley, and R. Seeger, Int. J. Quantum Chem. Symp. **10**, 1 (1976).
[59] R. Krishnan and J. A. Pople, Int. J. Quantum Chem. **14**, 91 (1978).
[60] R. Krishnan, M. J. Frisch, and J. A. Pople, J. Chem. Phys. **72**, 4244 (1980).
[61] K. Raghavachari, J. A. Pople, E. S. Replogle, and M. Head-Gordon, J. Phys. Chem. **94**, 5579 (1990).
[62] I. Shavitt, in *Modern Theoretical Chemistry*, edited by H. F. Schaefer III (Plenum, New York, 1977), Vol. 3, p. 189.
[63] B. R. Brooks and H. F. Schaefer, J. Chem. Phys. **70**, 5391 (1979).
[64] P. Saxe, D. J. Fox, H. F. Schaefer, and N. C. Handy, J. Chem. Phys. **77**, 5584 (1982).
[65] R. J. Bartlett, Annu. Rev. Phys. Chem. **32**, 359 (1981).
[66] G. D. Purvis III and R. J. Bartlett, J. Chem. Phys. **76**, 1910 (1982).
[67] J. Paldus, in *New Horizons of Quantum Chemistry*, edited by P.-O. Löwdin and B. Pullmann (Reidel, Dordrecht, 1983), p. 31.
[68] R. J. Bartlett, C. E. Dykstra, and J. Paldus, in *Advanced Theories and Computational Approaches to the Electronic Structure of Molecules*, edited by C. E. Dykstra (Reidel, Dordrecht, 1984), p. 127.
[69] G. E. Scuseria, A. C. Scheiner, T. J. Lee, J. E. Rice, and H. F. Schaefer, J. Chem. Phys. **86**, 2881 (1987).
[70] G. E. Scuseria, C. L. Janssen, and H. F. Schaefer, J. Chem. Phys. **89**, 7382 (1988).
[71] K. Raghavachari, G. W. Trucks, J. A. Pople, and M. Head-Gordon, Chem. Phys. Lett. **157**, 479 (1989).
[72] G. E. Scuseria and T. J. Lee, J. Chem. Phys. **93**, 5851 (1990).
[73] N. C. Handy, J. A. Pople, M. Head-Gordon, K. Raghavachari, and G. W. Trucks, Chem. Phys. Lett. **164**, 185 (1989).
[74] T. J. Lee, R. Kobayashi, N. C. Handy, and R. D. Amos, J. Chem. Phys. **96**, 8931 (1992).
[75] S. R. Langhoff and E. R. Davidson, Int. J. Quantum Chem. **8**, 61 (1974).
[76] C. L. Janssen, E. T. Seidl, G. E. Scuseria, T. P. Hamilton, Y. Yamaguchi, R. B. Remington, Y. Xie, G. Vacek, C. D. Sherrill, T. D. Crawford, J. T. Fermann, W. D. Allen, B. R. Brooks, G. B. Fitzgerald, D. J. Fox, J. F. Gaw, N. C. Handy, W. D. Laidig, T. J. Lee, R. M. Pitzer, J. E. Rice, P. Saxe, A. C. Scheiner, and H. F. Schaefer, PSI 2.0.8, PSITECH Inc., Watkinsville, GA, 1994.
[77] M. J. Frisch, G. W. Trucks, M. Head-Gordon, P. M. W. Gill, M. W. Wong, J. B. Foresman, B. G. Johnson, H. B. Schlegel, M. A. Robb, E. S. Replogle, R. Gomperts, J. L. Andres, K. Raghavachari, J. S. Binkley, C. Gonzalez, R. L. Martin, D. J. Fox, D. J. Defrees, J. Baker, J. J. P. Stewart, and J. A. Pople, GAUSSIAN 92, Revision A, Gaussian, Inc., Pittsburgh, PA, 1992.
[78] M. Dupuis, D. Spangler, and J. J. Wendolowski; modified by M. W. Schmidt, K. K. Baldridge, J. A. Boatz, J. H. Jensen, S. Koseki, M. S. Gordon, K. A. Nguyen, T. L. Windus, and S. T. Elbert, QCPE Bull. **10**, 52 (1990).
[79] J. F. Gaw and N. C. Handy, Annu. Rept. R. Soc. Chem. C **81**, 291 (1984).
[80] P. Jørgensen and J. Simons, *Geometrical Derivatives of Energy Surfaces and Molecular Properties* (Reidel, Dordrecht, 1986).
[81] H. F. Schaefer and Y. Yamaguchi, J. Mol. Struct. (Theochem) **135**, 369 (1986).
[82] A. C. Scheiner, G. E. Scuseria, J. E. Rice, and H. F. Schaefer, J. Chem. Phys. **87**, 5361 (1987).
[83] G. E. Scuseria, J. Chem. Phys. **94**, 442 (1991).
[84] Y. Osamura, Y. Yamaguchi, P. Saxe, M. A. Vincent, J. F. Gaw, and H. F. Schaefer, Chem. Phys. **72**, 131 (1982).
[85] Y. Osamura, Y. Yamaguchi, P. Saxe, D. J. Fox, M. A. Vincent, and H. F. Schaefer, J. Mol. Struct. (Theochem) **103**, 183 (1983).
[86] N. C. Handy, R. D. Amos, J. F. Gaw, J. E. Rice, and E. D. Simandiras, Chem. Phys. Lett. **120**, 151 (1985).
[87] E. D. Simandiras, N. C. Handy, and R. D. Amos, Chem. Phys. Lett. **133**, 324 (1987).
[88] The basic numerical differentiation formulas of various orders are given by A. G. Császár, in ''Anharmonic molecular force fields,'' *Encyclopedia of Computational Chemistry*, edited by P. v. R. Schleyer, N. L. Allinger, T. Clark, J. Gasteiger, P. Kollmann, and H. F. Schaefer III (Wiley, Chichester, 1997). The finite-difference schemes were implemented here with INTDIF, a general program for the numerical evaluation of force fields of various orders, written by Wesley D. Allen.
[89] T. J. Lee and P. R. Taylor, Int. J. Quantum Chem. Symp. **23**, 199 (1989).
[90] N. C. Handy, P. J. Knowles, and K. Somasundram, Theor. Chim. Acta **68**, 87 (1985).
[91] R. J. Bartlett and I. Shavitt, Chem. Phys. Lett. **50**, 190 (1977).
[92] W. D. Laidig, G. Fitzgerald, and R. J. Bartlett, Chem. Phys. Lett. **113**, 151 (1985).
[93] *JANAF Thermochemical Tables*, 3rd ed., J. Phys. Chem. Ref. Data **14**, Supp. No. 1 (1985).
[94] A. L. L. East and W. D. Allen, J. Chem. Phys. **99**, 4638 (1993).
[95] W. D. Allen, A. L. L. East, and A. G. Császár, in *Structures and Conformations of Non-Rigid Molecules*, edited by J. Laane, M. Dakkouri, B. van der Veken, and H. Oberhammer (Kluwer, Dordrecht, 1993), p. 343.
[96] N. L. Allinger, J. T. Fermann, W. D. Allen, and H. F. Schaefer, J. Chem. Phys. **106**, 5143 (1997).
[97] B. D. Wladkowski, W. D. Allen, and J. I. Brauman, J. Phys. Chem. **98**, 13532 (1994).
[98] S. J. Klippenstein, A. L. L. East, and W. D. Allen, J. Chem. Phys. **105**, 118 (1996).
[99] UHF-based results are used here because restricted-orbital (RHF) capabilities for BD(TQ) computations on open-shell species have yet to be developed. This choice is justified by a striking level of agreement between RHF- vs UHF-orbital high-order correlated predictions of ΔE_e for these reactions. For example, the cc-pVDZ RCCSD(T) and UCCSD(T) results for $\Delta E_e(2)$ are -133.30 and -133.16 kcal mol^{-1}, respectively.
[100] I. M. Mills, in *Molecular Spectroscopy: Modern Research*, edited by K. N. Rao and C. W. Mathews (Academic, New York, 1972), Vol. 1, p. 115; D. Papoušek and M. R. Aliev, *Molecular Vibrational-Rotational Spectra* (Elsevier, Amsterdam, 1982); D. A. Clabo, Jr., W. D. Allen, R. B. Remington, Y. Yamaguchi, and H. F. Schaefer, Chem. Phys. **123**, 187 (1988).
[101] The size of this defect is surely a consequence of the limited applicability of a perturbation-theory analysis in treating the ν_3 vibration. In this regard it is noteworthy that the effective empirical parameters $\alpha_3^B = 0.005\,57$ and $\alpha_3^C = 0.007\,64$ cm^{-1} (Refs. 26, 27) are considerably smaller than the corresponding constants in Table X.
[102] To estimate the effect of core correlation on the bond distances of SiC_2, geometry optimizations were performed for the lowest singlet state of $C_2(^1\Sigma_g^+)$ and $SiC(^1\Sigma^+)$ with the CCSD(T) method using a completely uncontracted cc-pVTZ primitive basis augmented with a tight $(1p,1d,1f)$ shell, the exponents of which were obtained by multiplying by 3.0 the largest exponent of that particular angular momentum in the original basis and rounding to the nearest half-integer. This basis is similar to those constructed by Martin and Taylor (Refs. 103, 104) for studying the effects of core correlation. The equilibrium bond distances obtained with frozen core orbitals were 1.2451 Å for C_2 and 1.8358 Å for SiC, and the corresponding distances were 1.2420 and 1.8314 Å when all electrons were correlated. The inclusion of core correlation thus shortens the C–C and Si–C bonds by 0.0031 and 0.0044 Å, respectively.
[103] J. M. L. Martin, Chem. Phys. Lett. **242**, 343 (1995).
[104] J. M. L. Martin and P. R. Taylor, Chem. Phys. Lett. **225**, 473 (1994).
[105] A. G. Császár and W. D. Allen, J. Chem. Phys. **104**, 2746 (1996).
[106] C. W. Bauschlicher, Jr. and H. Partridge, J. Chem. Phys. **100**, 4329 (1994).